

1 **Interactive comment on “New particle formation events observed at**  
2 **King Sejong Station, Antarctic Peninsula – Part 1: Physical**  
3 **characteristics and contribution to cloud condensation nuclei” by**  
4 **Jaeseok Kim et al.**

5  
6 **Anonymous Referee #1**

7  
8 Received and published: 18 December 2018

9  
10 We thank Referee 1 for providing insightful suggestions that have considerably improved the readability of the  
11 revised manuscript. Our responses to general and specific comments raised by Referee 1 are stated below. The  
12 revised manuscript was uploaded in the form of a supplement

13  
14 General comments:

15 The manuscript at hand characterizes new particle formation (NPF) events observed at the Korean Antarctic  
16 Station King Sejong. As the authors state, this is the first NPF investigation from the Antarctic Peninsula. To  
17 my knowledge it is based on the longest observation period actually measured in Antarctica regarding this topic.  
18 In addition, the authors discussed in particular NPF events along with cloud condensation nuclei (CCN) data.  
19 The article is written in a straight and concise way and presents invaluable results to elucidate NPF and its  
20 impact on CCN availability at this site and (coastal) Antarctica in general. However, the article in the present  
21 appearance has some weak points. Especially the regrettably scarce discussion in general is not commensurate  
22 with the unquestionable valuable data set. In addition, description of the used instruments and data evaluation  
23 procedures are often insufficient (see specific comments below). I think this outstanding data set is worth the  
24 effort addressing this weakness and considering a more in-depth discussion. Notwithstanding, I am confident  
25 that the data and their evaluation presented here are of high quality and on the whole, the subject is appropriate  
26 to ACP. Hence, I recommend accepting the paper after revisions according to my specified suggestions from  
27 above and listed below.

28  
29 Specific comments:

30 1. The authors should provide specification and operation details for the SMPS and CCN instruments even  
31 though they were comparable to Kim et al. (2017). Furthermore, I miss an adequate presentation of the SMPS  
32 results! In any case, it would be advisable to show some figures (e.g. the typical  $D_p$  vs. time contour plots), at  
33 least for the two case “A” NPF events.

34  
35 Authors' response: We have described the specification and operation details for the SMPS and CCN system in  
36 our previous paper (Kim et al., 2017). Following referee's advice, in the revised manuscript, we modified the  
37 paragraph on Page 4 Line 5 to clarify the specification and operation details for the SMPS and CCN instruments.

38  
39 *“The aerosol size distributions of particles ranging from 10 to 300 nm were measured every 3 minutes with a*  
40 *scanning mobility particle sizer (SMPS) consisting of a differential mobility analyzer (DMA; HCT Inc., LDMA*  
41 *4210) and a CPC (TSI 3772). The flow rate of sheath air and aerosol flow of DMA were  $10 \text{ L min}^{-1}$  and  $1 \text{ L min}^{-1}$ ,*  
42 *respectively. The CCN concentrations were simultaneously measured by using a CCN counter (DMT CCN-*  
43 *100) with five different supersaturation values (i.e. 0.2, 0.4, 0.6, 0.8 and 1.0%). The sampling duration was set*  
44 *to be 5 minutes for each supersaturation value (except for 0.2%). For the 0.2% supersaturation value, the CCN*  
45 *concentration was measured for 10 min because of stability after measurements at 1% supersaturation value.*  
46 *In the present work, only results of CCN concentration for a 0.4% supersaturation value were used.”*

47  
48  
49 We also added following contour figures in the revised manuscript.

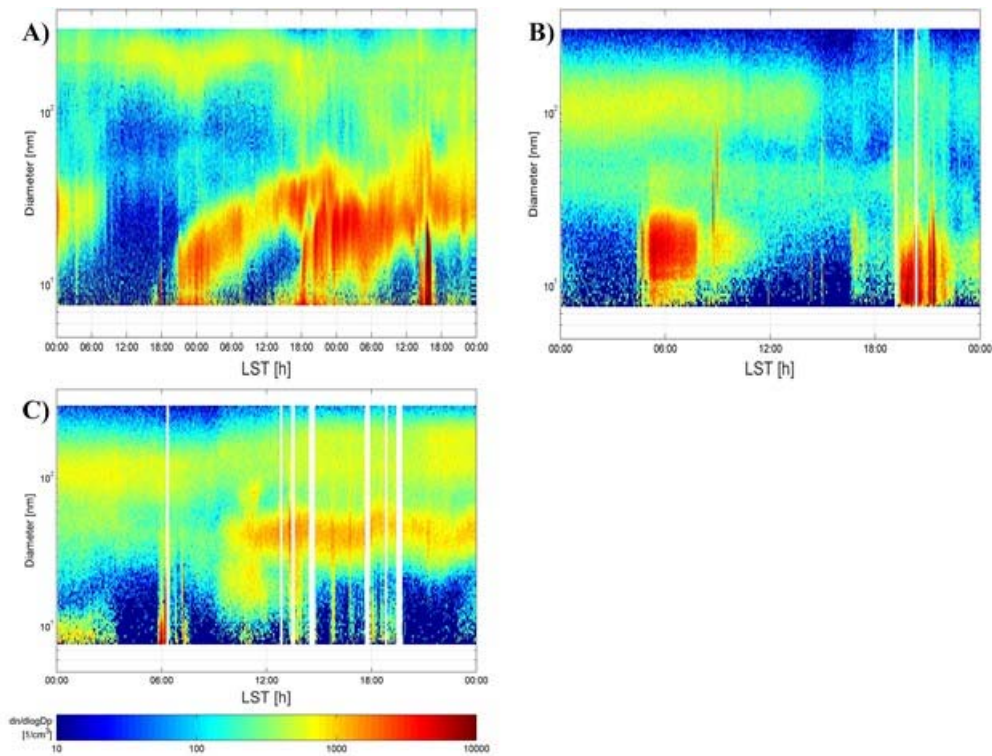


Figure 1. Example of types of the NPF based on the SMPS data. (a) type A (18 January 2011-20 January 2011), (b) type B (13 January 2015) and (c) type C (9 January 2015). Type A is days when the formation and growth of nanoparticles should be clear. Type B is days when the formation occurred but growth was not clear. Type C is days when it cannot be said whether there is an event or not.

2. Another concern is the lack of an appropriate CCN data presentation. For instance, the authors showed no figures regarding the CCN spectrum. I would appreciate a thorough description of the performed data analysis.

Authors' response: CCN data were obtained at five different supersaturation ratio values (0.2, 0.4, 0.6, 0.8 and 1.0%) using commercial CCNC (DMT CCN-100). The sampling time was set at 5 min including stability duration for each supersaturation value except for 0.2% supersaturation value. For 0.2% supersaturation value, the CCN data was collected for 10 min because the additional time was needed to achieve stability after measurements at 1.0% supersaturation value. Based on previous study (Anttila et al., 2012) which compared relationship between CCN concentration and cloud droplet number concentration, in this study, hourly mean CCN data at 0.4% supersaturation value were used. Based on this results, we compared variation in normalized values of  $CN_{2.5-10}$  and CCN concentrations during NPF period as shown in Figure 2.

To explain method for CCN data analysis, we added the following sentence in Page 4 Line 8:

*“The CCN concentrations were simultaneously measured by using a CCN counter (DMT CCN-100) with five different supersaturation values (i.e. 0.2, 0.4, 0.6, 0.8 and 1.0%). The sampling duration was set to be 5 minutes for each supersaturation value (except for 0.2%). For the 0.2% supersaturation value, the CCN concentration was measured for 10 min because of stability after measurements at 1% supersaturation value. In the present work, only results of CCN concentration for a 0.4% supersaturation value were used.”*

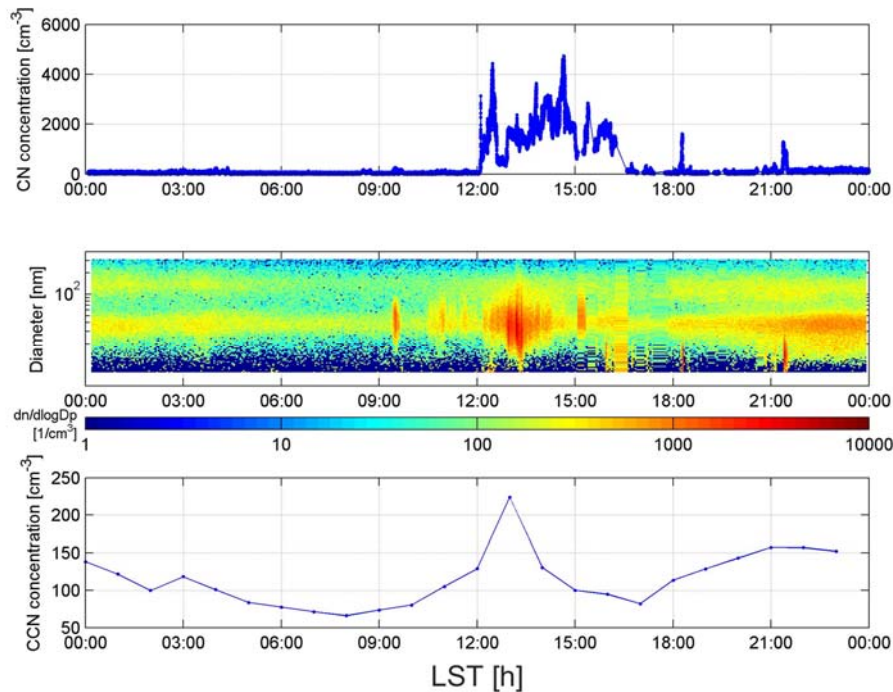


Figure 2. Example of comparison among CN concentrations from CPC data (upper panel), size distribution from SMPS data (middle panel) and hourly mean CCN concentration (bottom panel) at 0.4% supersaturation value as a function of time on 30 March 2009.

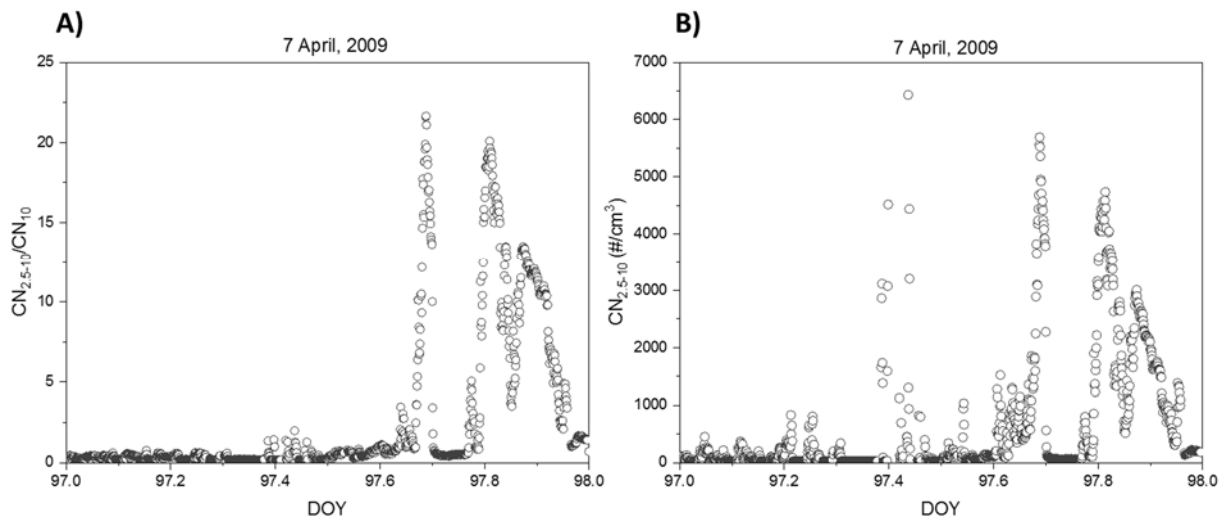
Chapters 2.2.1. and 2.2.2: The authors based their definition and classification of NPF events on the criteria compiled by Dal Maso et al. (2005) and Yli-Juuti et al. (2009), which are widely accepted by the community. According to these previous studies, an NPF event must show signs of growth (see Dal Maso et al., 2005, p. 326). Therefore, NPF events can only be identified by size distribution (here SMPS) data, but clearly not by sole CN<sub>2.5</sub> minus CN<sub>10</sub> data. The latter just indicate a potential NPF, which may be better termed as particle burst.

Authors' response: According to previous study (Dal Maso et al., 2005), an NPF event must show signs of growth. Authors acknowledge and agree that the SMPS data are widely used for identification and classification of the NPF events. However, in this study, because the availability of SMPS data set was lower than that of CPC data set, CN<sub>2.5</sub> and CN<sub>10</sub> data were used to define NPF events and SMPS data used to classify types of the NPF events. For identification of the NPF events, CN<sub>2.5-10</sub> data, CN<sub>2.5-10</sub>/CN<sub>10</sub> data and the duration time data were used as mentioned at Section 2.2.1. In particular, CN<sub>2.5-10</sub>/CN<sub>10</sub> values can be used to distinguish newly formed particles to background particles (Warren and Seinfeld, 1985; Covert et al., 1992; Humphries et al., 2015). Since we used strict category to define the burst of nanoparticles, this supports the widely-used definition of the NPF events. Authors think the definition of the NPF event is feasible in this study.

Chapters 2.2.3: I guess that CN and especially CN<sub>2.5</sub> – CN<sub>10</sub> concentration data based on 1 s resolution are highly fluctuating, making the FR evaluation somewhat arbitrary. Please specify in more detail the way you extract  $\text{dNnuc}/\text{dt}$  from the data (maybe by showing a representative figure?).

Authors' response: Authors appreciate the issue raised by the referee. Because CN data with 1 s time resolution are highly fluctuating, FR was estimated using an one-minute averaged CN concentration. To calculate the FR values, we first checked CN<sub>2.5-10</sub>/CN<sub>10</sub> values. The CN<sub>2.5-10</sub>/CN<sub>10</sub> values can be used to distinguish between newly formed particles and background particles events (Warren and Seinfeld, 1985; Covert et al., 1992; Humphries et al., 2015). As shown in Figure 3, when CN<sub>2.5-10</sub>/CN<sub>10</sub> values were higher than 10, we considered

1 as NPF events as mentioned Sec 2.2.1. Time variation (dt) was estimated from the time it starts to increase of  
2  $CN_{2.5-10}/CN_{10}$  to the time it was highest values. Variation of  $CN_{2.5-10}$  concentration ( $dN_{nuc}$ ) was calculated at  
3 that time.  
4  
5



6  
7 Figure 3. Example for estimation of the formation rate during NPF event on 7 April 2009: (a)  $CN_{2.5-10}/CN_{10}$  and  
8 (b)  $CN_{2.5-10}$  concentration with 1 min time resolution.  
9

10 To clarify we modified sentence to following text on Page 6 Line 2:  
11 “On the basis of the average number concentration data with 1 min time resolution, the FR was calculated for  
12 cases in which  $CN_{2.5-10}/CN_{10}$  values and  $CN_{2.5-10}$  concentrations sharply increased (Fig. S1 in the Supplement).”  
13

14 Chapters 2.3: Please specify, in which way/procedure you have characterized air masses (by cluster analysis or  
15 just “manually”)?  
16

17 Authors’ response: Air mass backward trajectory analysis during the NPF event periods was conducted by using  
18 the HYSPLIT model (<http://www.arl.noaa.gov/HYSPLIT.php>). The origin of air masses arriving at the  
19 observation site during the NPF events (a total of 101 event days) was manually categorized into four cases by  
20 analyzing 48-h backward trajectory data ending at height of 100m, 500m and 1500 m above the ground level.  
21 For instance, if time of the NPF events was from 13:00 to 17:00, we run the 48-h air mass backward trajectory  
22 for each hour. The results with similar air mass origins and pathways during the NPF event periods at three  
23 different heights were used for the analysis in this study.  
24

25 To clarify we modified paragraph to following text on Page 8 Line 1:  
26 “The origin of air masses arriving at the observation site during the NPF events (a total of 101 event days) was  
27 manually categorized into four cases by analyzing 48-h backward trajectory data ending at height of 100, 500  
28 and 1500 m above the ground level. The results with similar air mass origins and pathways during the NPF  
29 event periods at three different heights were used for the analysis in this study, as shown in Fig. 2”  
30

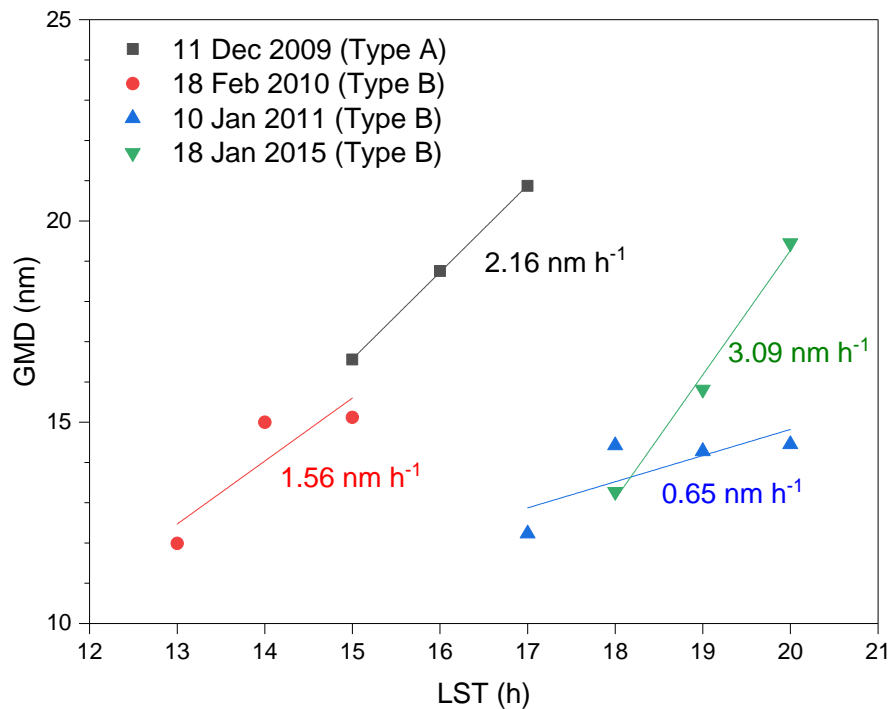
31 Results and Discussion chapter and Tables 4 and 5: The authors observed just two type “A” NPF events, from  
32 which growth can be determined with confidence according to Dal Maso et al. (2005). For type “B” events, the  
33 authors state that growth was not clear (see caption of table 4). I am confused about this: Does this mean the  
34 bottom line is that the reported growth rates were based on merely two events? Please clarify this point!  
35

36 Authors’ response: Aerosol size distribution data were used for classification of the NPF events. Based on the  
37 contour plots of aerosol size distribution, type of the NPF events was classified. For the calculation of growth  
38 rates, hourly mean aerosol size distribution data was used for all types of NPF. The geometric mean diameter  
39 (GMD) of particles which is limited to the size range of 10-25 nm was used. According to these method, growth

1 rate of particles ranging from 10 to 25 nm was estimated regardless of type of the NPF events as shown in  
2 Figure 4.

3  
4 To clarify we modified paragraph to following text on Page 6 Line 16:

5 “Based on the hourly mean aerosol size distribution data, the geometric mean diameter (GMD) of particles  
6 which is limited to the size range of 10-25 nm was used. Here, the GMD was calculated from log-normal fitting  
7 analysis. According to these method, growth rate of particles ranging from 10-25 nm was estimated regardless  
8 of the NPF event types (Fig. S2 in the Supplement)”  
9



10  
11 Figure 4. Geometric mean diameter (GMD) of particles ranging from 10 nm to 25 nm as a function of the time:  
12 the growth rate (nm h<sup>-1</sup>) was calculated as the regression slope. The LST means local standard time.

13  
14 Chapter 3.3: From my point of view the presented discussion is inadequate. Evaluation of the CCNC data  
15 demands a more detailed description and discussion. Especially: A systematic analysis along with SMPS data  
16 would be crucial and should be presented. Are your CCNC results consistent with SMPS data?  
17

18 Authors' response: As described in section 3.3, according to previous studies (Pierce et al., 2014; Shen et al.,  
19 2016; Rose et al., 2017), in order to understand relationship between NPF event and CCN concentration, it was  
20 suggested that number concentrations of particles larger than 50, 80 and 100 nm estimated by SMPS data are  
21 compared with aerosol size distribution data. While, in this study, CCN concentration measured directly by  
22 CCN counter were compared concentration of newly formed particles (CN<sub>2.5-10</sub>) as the function of time during  
23 NPF event periods. Since it was very rare when the all 3 instruments – CPCs, SMPS, and CCN counter – are  
24 running together with the very best condition during the particle burst event, authors decide to choose the best  
25 way available, comparing CPC data with CCN during the 34 days with two dataset are available. In this  
26 manuscript, authors want to show the results that the CCN concentration increase are noticed for a couple of  
27 hours following NPF event under clean Antarctic environment, and this results are derived directly from in-situ  
28 CCN measurements.  
29  
30

31 Chapter 3.4, lines 12 through 14: The authors argue that higher GR observed in air masses emerging from the  
32 Bellinghousen Sea area are due to higher source rates of condensable vapour. Unless I am very much mistaken,  
33 this is a typical case of circular reasoning, because regarding eqs. (4) and (5), the source rate Q is linearly

1 dependent on the GR, isn't it!  
2  
3 Authors' response: The referee pointed out correctly. To clarify we modified sentence to following text on Page  
4 12 Line 20:  
5  
6 *"However, in case of the air mass originating from the Bellingshausen Sea (Case IV), the GR was relatively*  
7 *higher than the values of air masses originated from other region."*  
8  
9  
10 Technical corrections:  
11 Page 1 (abstract), line 16: Misleading phrase. Change to " : :during particle bursts (not during a particle burst): : :"  
12  
13 Authors' response: We changed it (Page 1 Line 16).  
14  
15  
16 Page 1 (abstract), lines 23, 27, and throughout the text: Please present measured values and values derived from  
17 data just with their relevant/meaningful digits.  
18  
19 Authors' response: Thanks! We modified it (Page 1 Line 23; Page 1 Line 27).  
20  
21  
22 Page 3, line 3: Misleading phrase. Change to "A NPF event occurring in the period between December 1998  
23 and December 2000: : :"  
24  
25 Authors' response: We changed it (Page 3 Line 3).  
26  
27  
28 Page 4, line 15: Modify to " : :raw data measured during the following conditions: : :"  
29  
30 Authors' response: We changed it (Page 4 Line 22).  
31  
32  
33 Page 4, line 21 and throughout the manuscript: Delete "value" in "value difference".  
34  
35 Authors' response: We modified it (Page 5 Line 8).  
36  
37  
38 Page 5, line 24: Use a unique consistent term for particle number concentrations between 2.5 nm and 10 nm  
39 (either CN<sub>2.5-10</sub> or CN<sub>2.5</sub> – CN<sub>10</sub>) throughout the text!  
40  
41 Authors' response: Thanks! We used CN<sub>2.5-10</sub> in the revised manuscript (Page 5 Line 9; Page 5 Line 11; Page 5  
42 Line 12; Page 5 Line 13; Page 5 Line 15).  
43  
44  
45 Page 6, line 15: "speed" should be "loss rate".  
46  
47 Authors' response: We changed it (Page 6 Line 25).  
48  
49  
50 Page 8, line 15: "should speculate" should be "indicates".  
51  
52 Authors' response: We changed it (Page 9 Line 1).  
53  
54

1 Page 9, line 18: Delete “(which is undefined days)”.

2

3 Authors’ response: We deleted it.

4

5

6 Page 9, line 23: Delete “whereas”.

7

8 Authors’ response: We deleted it.

9

10

11 Page 11, line 18-21: I do not understand the meaning of this phrase - please clarify: What is meant with  
12 “undefined case” here? Delete this line in Table 5.

13

14 Authors’ response: We agree reviewer’s opinion. We removed “undefined case” in Table 5 and text in the  
15 manuscript.

16

17

18 Page 12, line 2: “: : :a indicate decline: : :” should be “: : :indicate a decline: : :”

19

20 Authors’ response: We changed it (Page 12 Line 16).

21

22

23 Page 12, line 3: “: : :discussed: : :” should be “: : :discussing: : :”

24

25 Authors’ response: We changed it (Page 12 Line 18).

26

27

28 Page 12, line 4: “: : :simulation: : :” should be “: : :model: : :”

29

30 Authors’ response: We changed it (Page 12 Line 19).

31

32

33 Page 12, line 7: Misleading phrase. The term “estimates of the biological characteristics” is somewhat vague,  
34 please specify.

35

36 Authors’ response: We have replaced “estimates of the biological characteristics” to “estimates of the biological  
37 activities” (Page 12 Line 21)

38

39

40 Page 12, lines 8-9: DMS oxidation to sulphuric acid occurs in the atmosphere but not in the ocean – please  
41 correct!

42

43 Authors’ response: We have replaced “oxidation of DMS in oceans” to “oxidation of DMS emitted from oceans”  
44 (Page 12 Line 23)

45

46 Reference

47 Anttila, T., Brus, D., Jaatinen, A., Hyvärinen, A. P., Kivekäs, N., Romakkaniemi, S., Komppula, M., and  
48 Lihavainen, H.: Relationships between particles, cloud condensation nuclei and cloud droplet activation  
49 during the third Pallas Cloud Experiment, Atmos. Chem. Phys., 12, 11435-11450, 10.5194/acp-12-11435-  
50 2012, 2012.

51 Covert, D. S., Kapustin, V. N., Quinn, P. K., and Bates, T. S.: New particle formation in the marine boundary  
52 layer, J. Geophys. Res., 97, 20581, doi:10.1029/92JD02074, 1992.

1  
2 **New particle formation observed at King Sejong Station, Antarctic**  
3 **Peninsula – Part 1: Physical characteristics and contribution to cloud**  
4 **condensation nuclei**

5  
6 Jaeseok Kim<sup>1,2</sup>, Young Jun Yoon<sup>1,\*</sup>, Yeontae Gim<sup>1</sup>, Jin Hee Choi<sup>1</sup>, Hyo Jin Kang<sup>1,3</sup>, Ki-Tae Park<sup>1</sup>,  
7 Jiyeon Park<sup>1</sup>, and Bang Yong Lee<sup>1</sup>

8  
9 <sup>1</sup>Korea Polar Research Institute, 26 Songdomirae-ro, Yeonsu-gu, Incheon 21990, Republic of Korea

10 <sup>2</sup>Korea Research Institute of Standards and Science, 267 Gajeong-ro, Yuseong-gu, Daejeon 34113,  
11 Republic of Korea

12 <sup>3</sup>University of Science & Technology (UST), 217 Gajeong-ro, Yuseong-gu, Daejeon 34113, Republic  
13 of Korea

14 \*Correspondence to: Young Jun Yoon (yjyoon@kopri.re.kr)

15  
16 **Abstract**

17 The physical characteristics of aerosol particles during particle bursts observed at King Sejong  
18 Station in Antarctic Peninsula from March 2009 to December 2016 were analyzed. This study focuses  
19 on the seasonal variation in parameters related to particle formation such as the occurrence, formation  
20 rate (FR) and growth rate (GR), condensation sink (CS), and source rate of condensable vapor. The  
21 number concentrations during new particle formation (NPF) events varied from 1707 cm<sup>-3</sup> to 83120  
22 cm<sup>-3</sup>, with an average of 20649 ± 9290 cm<sup>-3</sup>, and the duration of the NPF events ranged from 0.6 h to  
23 14.4 h, with a mean of 4.6 ± 1.5 h. The NPF event dominantly occurred during austral summer period  
24 (~72%). The measured mean values of FR and GR of the aerosol particles were 2.79 ± 1.05 cm<sup>-3</sup> s<sup>-1</sup>  
25 and 0.68 ± 0.27 nm h<sup>-1</sup>, respectively showing enhanced rates in the summer season. The mean value  
26 of FR at King Sejong Station was higher than that at other sites in Antarctica, at 0.002-0.3 cm<sup>-3</sup> s<sup>-1</sup>,  
27 while those of growth rates was relatively similar results observed by precious studies, at 0.4~4.3 nm  
28 h<sup>-1</sup>. The derived average values of CS and source rate of condensable vapor were (6.04 ± 2.74) × 10<sup>-3</sup>  
29 s<sup>-1</sup> and (5.19 ± 3.51) × 10<sup>4</sup> cm<sup>-3</sup> s<sup>-1</sup>, respectively. The contribution of particle formation to cloud



1 condensation nuclei (CCN) concentration was also investigated. The CCN concentration during the  
2 NPF period increased approximately 9% compared with the background concentration. In addition,  
3 the effects of the origin and pathway of air masses on the characteristics of aerosol particles during a  
4 NPF event were determined. The FRs were similar regardless of the origin and pathway, whereas the  
5 GRs of particles originating from the Antarctic Peninsula and the Bellingshausen Sea, at  $0.77 \pm 0.25$   
6  $\text{nm h}^{-1}$  and  $0.76 \pm 0.30 \text{ nm h}^{-1}$ , respectively, were higher than those of particles originating from the  
7 Weddell Sea ( $0.41 \pm 0.15 \text{ nm h}^{-1}$ ).

8

## 9 **1. Introduction**

10 Understanding the effect of atmospheric aerosol particles on climate change is an important issue  
11 in atmospheric science. These particles are highly significant substances in the radiation transfer  
12 process in the atmosphere, with direct effects through scattering and absorption of solar radiation and  
13 indirect effects by acting as cloud condensation nuclei (CCN) for cloud droplets (Anttila et al., 2012).  
14 These particles also influence the properties and life time of clouds (Twomey, 1977; Albrecht, 1989).  
15 Although aerosol particles play an important role in global and regional climates, large uncertainties  
16 remain owing to a lack of knowledge on their formation and physicochemical characteristics (Carslaw  
17 et al., 2013; IPCC, 2013).

18 New particle formation (NPF) frequently occurs in the atmosphere and leads to enhancement of the  
19 total number concentrations of aerosol particles due to high numbers of nucleation mode particles  
20 (Spracklen et al., 2006; Dall'Osto et al., 2017). The modeling study of Pierce and Adams (2007)  
21 indicates that ultrafine particles of  $<100 \text{ nm}$  can contribute to maximum CCN generations of 40% and  
22 90% at the boundary layer and in the remote free troposphere, respectively. In order to understand the  
23 characteristics of the NPF, studies have been conducted in various regions including coastal, forest,  
24 mountainous, rural and urban sites (O'Dowd et al., 2002; Komppula et al., 2003; Kulmala et al., 2004;  
25 Yoon et al., 2006; Park et al., 2009; Kim et al., 2011; Rose et al., 2015; Bianchi et al., 2016; Kontkanen

1 et al., 2017). In addition, studies on the NPF phenomenon have recently been conducted at various  
2 sites in the polar regions (Asmi et al., 2010; Järvinen et al., 2013; Kyrö et al., 2013; Park et al., 2004;  
3 Weller et al., 2015; Humphries et al., 2016; Nguyen et al., 2016; Willis et al., 2016; Barbaro et al.,  
4 2017; Dall'Osto et al., 2017). A NPF event occurring in the period between December 1998 and  
5 December 2000 at the South Pole was reported by Park et al. (2004). Kyrö et al. (2013) showed that  
6 oxidized organics derived from the oxidation of biogenic precursors originating from local melting  
7 ponds might have contributed to particle growth at the Finnish research station Aboa (73.50°S,  
8 13.42°W). Although CCN concentrations were indirectly estimated at Aboa, Asmi et al. (2010) also  
9 showed and discussed hygroscopic growth factor and CCN activity. In addition, studies on the NPF  
10 were conducted at the Concordia station, Dome C (75.10°S, 123.38°E; Järvinen et al., 2013) and at the  
11 coastal Antarctic station Neumayer (70.65°S, 8.25°W; Weller et al., 2015). Although studies on NPF  
12 events have been conducted at various stations in the Antarctica, no results are available for the station  
13 in the Antarctic Peninsula. Also, the contribution of NPF to CCN concentration is not well understood  
14 in this area. Furthermore, results of the general long-term characteristics of aerosol particles during the  
15 period of NPF observation in Antarctica are rare compared with those in other continents.

16 In the present study, the frequency of NPF events was determined on the basis of total aerosol  
17 number concentration. We investigated the physical characteristics such as formation rate (FR) and  
18 growth rate (GR), condensation sink (CS) and source of condensation vapor as well as the seasonality  
19 of atmospheric aerosols during NPF events at King Sejong Station in the Antarctic Peninsula. The  
20 effect of particle formation on CCN concentrations was also examined. Furthermore, the air mass back  
21 trajectories were analyzed by using the Hybrid Single Particle Lagrangian Integrated Trajectory  
22 (HYSPLIT) model to understand physical properties of NPF events depending on the origins and  
23 pathway of the air masses.

## 24 25 **2. Methods**

## 1 **2.1. Site description and instrumentation**

2 The data analyzed in this study were obtained from March 2009 to December 2012 at the King  
3 Sejong station in the Antarctic Peninsula (62.22°S, 58.78°W). Further details on the sampling site as  
4 well as the instrumental specification and operation were introduced in the previous study (Kim et al.,  
5 2017). In brief, two condensation particle counters (CPCs; TSI 3776 and TSI 3772) were used to  
6 measure the total particle number concentrations. The aerosol size distributions of particles ranging  
7 from 10 to 300 nm were measured every 3 minutes with a scanning mobility particle sizer (SMPS)  
8 consisting of a differential mobility analyzer (DMA; HCT Inc., LDMA 4210) and a CPC (TSI 3772).  
9 The flow rate of sheath air and aerosol flow of DMA were 10 L min<sup>-1</sup> and 1 L min<sup>-1</sup>, respectively. The  
10 CCN concentrations were simultaneously measured by using a CCN counter (DMT CCN-100) with  
11 five different supersaturation values (i.e. 0.2, 0.4, 0.6, 0.8 and 1.0%). The sampling duration was set  
12 to be 5 minutes for each supersaturation value (except for 0.2%). For the 0.2% supersaturation value,  
13 the CCN concentration was measured for 10 min because of stability after measurements at 1%  
14 supersaturation value. In the present work, only results of CCN concentration for a 0.4%  
15 supersaturation value were used. In addition, meteorological parameters including temperature,  
16 relative humidity, wind speed, wind direction, pressure, and solar radiation intensity were continuously  
17 monitored by using an automatic weather station (AWS; Vaisala HMP45 for measuring temperature  
18 and relative humidity, WeatherTronics 2102 for measuring wind speed and direction, WeatherTronics  
19 7100 for measuring pressure and Eppley Precision Spectral Pyranometer PSP for measuring solar  
20 radiation intensity) system.

## 21 22 **2.2. Data analysis**

23 To ensure data quality, raw data measured during the following conditions were discarded: (i) wind  
24 direction between 355° and 55° (local pollution sector) (ii) concentration of black carbon higher than  
25 100 ng m<sup>-3</sup>, (iii) wind speed less than 2 m s<sup>-1</sup> and (iv) instrument malfunction based on the log-book.

1 If valid data for one day were less than 50% after discarding the raw data, such days were excluded.  
2 The acquisition rate for each instrument is summarized in Table 1. Here, the acquisition rate indicates  
3 the value of the analyzed days divided by the total measurement days. Because the acquisition rate  
4 from the SMPS was lower than that of the CPC in this study, the value difference between the  
5 concentrations of particles larger than 2.5 nm ( $CN_{2.5}$ ) and 10 nm ( $CN_{10}$ ) observed from two CPCs was  
6 used to identify the NPF events.

### 7 8 **2.2.1. Definition of NPF events**

9 As mentioned in the previous section, the **difference** between  $CN_{2.5}$  and  $CN_{10}$  concentrations were  
10 used to define days for NPF events or non-NPF events (Yoon et al., 2006). **The  $CN_{2.5-10}$  represents** the  
11 number concentrations of newly formed particles produced from gas-to-particle conversion. The NPF  
12 days were defined in this study according to the following conditions: (i) The  $CN_{2.5-10}$  is higher than  
13  $500 \text{ cm}^{-3}$  (ii) the  $CN_{2.5-10}/CN_{10}$  ratio is higher than 10 and (iii) the NPF duration is longer than 30 min.  
14 **The  $CN_{2.5-10}/CN_{10}$  ratio is the parameter used to distinguish between particles newly formed from gas-**  
15 **to-particle conversion and background particles (Warren and Seinfeld, 1985; Humphries et al., 2015).**  
16 Humphries et al. (2016) also used the  $CN_{2.5-10}/CN_{10}$  ratio to distinguish the NPF days during a 52 days'  
17 voyage in the East Antarctic sea ice region because the number concentration data were more reliable  
18 than the size distribution data.

### 19 20 **2.2.2. Classification of NPF events using SMPS data**

21 After identification of the NPF event days, classification of the NPF events was conducted by using  
22 size distributions from a SMPS. The NPF events were classified into three types of A, B and C  
23 according to the classification by Dal Maso et al. (2005) and Yli-Juuti et al. (2009) as shown in Fig. 1.  
24 Type A describes days in which the formation and growth of particles were clear. Type B describes  
25 days in which the formation occurred but growth was not clear. Type C describes days in which the  
26 event occurrence was not distinct.

### 2.2.3. Estimation of parameters for NPF characteristics

On the basis of the average number concentration data with 1 min time resolution, the FR was calculated for cases in which  $CN_{2.5-10}/CN_{10}$  values and  $CN_{2.5-10}$  concentrations sharply increased (Fig. S1 in the Supplement). The FR of new particles ranging from 2.5 nm to 10 nm was determined according to variation in the number concentrations of  $CN_{2.5-10}$  based on the following equation (Dal Maso et al., 2005):

$$FR = \frac{dN_{nuc}}{dt} + F_{coag} + F_{growth} \quad (1)$$

Here,  $N_{nuc}$  is the particle number concentrations of nucleation mode. In this study, the  $CN_{2.5-10}$  concentrations obtained by two particle counters were used for the term  $N_{nuc}$ .  $F_{coag}$  is the particle loss in accordance with coagulation, and  $F_{growth}$  represents the flux of particles growing from the nucleation mode. Because the  $CN_{2.5-10}$  concentrations were predominant in the total number concentration and the particles rarely grew over the nucleation mode during the formation period, the  $F_{coag}$  and  $F_{growth}$  terms in Eq. 1 were neglected in this study (Dal Maso et al., 2005; Shen et al., 2016).

The GRs were calculated by using the size distributions measured by a SMPS. Based on the hourly mean aerosol size distribution data, the geometric mean diameter (GMD) of particles which is limited to the size range of 10-25 nm was used. Here, the GMD was calculated from log-normal fitting analysis. According to these method, growth rate of particles ranging from 10-25 nm was estimated regardless of the NPF event types (Fig. S2 in the Supplement). The GR was determined by rate of change in the GMD by using the following equation (Kulmala et al., 2004; Dal Maso et al., 2005):

$$GR = \frac{dD_p}{dt} \quad (2)$$

1 The CS is an important parameter governing the NPF because it indicates [the loss rate](#) in which  
2 gaseous molecules condense onto pre-existing aerosols. It can be estimated from the size distribution  
3 data according to the following equation (Dal Maso et al., 2005; Kulmala et al., 2005; Shen et al.,  
4 2016):

$$5 \quad CS = 2\pi D \sum_{dp} \beta_m d_p N_{dp} \quad (3)$$

7 where  $D$  is the diffusion coefficient of the condensable vapor,  $\beta$  is the transitional regime correction  
8 factor from Fuchs and Sutugin (1970), and  $d_p$  and  $N_{dp}$  are the particle size and number concentration,  
9 respectively. It is assumed that condensable vapor is gaseous sulfuric acid which has been reported to  
10 play an important role in the nucleation process (Dal Maso et al., 2005).

12 According to the GR and the CS, it is possible to estimate condensable vapor concentration,  $C_v$  (unit:  
13 molecules  $\text{cm}^{-3}$ ) and its source rate,  $Q$  (unit: molecules  $\text{cm}^{-3} \text{ s}^{-1}$ ; Kulmala et al., 2001; Dal Maso, 2002),  
14 assuming that the particle growth is caused by condensation of a low volatile vapor to the particle  
15 surface. In the nucleation mode, the relationship between  $C_v$  and GR is estimated by the following  
16 equation:

$$17 \quad C_v = A \times GR \quad (4)$$

19 where  $A$  is a constant, specifically  $1.37 \times 10^7 \text{ h cm}^{-3}$  for a vapor with the molecular properties of sulfuric  
20 acid. It assumed that  $C_v$  is constant during the growth process.

22 Assuming no other sink terms for the condensing vapor, source rate of condensable vapor is  
23 estimated under the steady-state condition:

$$24 \quad Q = CS \times C_v \quad (5)$$

### 26 **2.3. Backward trajectory analysis**

1 To understand characteristics of NPF events depending on the origin and pathway of air masses, air  
2 mass backward trajectory analysis was performed by using the HYSPLIT model (Stein et al., 2015;  
3 <http://www.arl.noaa.gov/HYSPLIT.php>). The origin of air masses arriving at the observation site  
4 during the NPF events (a total of 101 event days) was manually categorized into four cases by  
5 analyzing 48-h backward trajectory data ending at height of 100, 500 and 1500 m above the ground  
6 level. The results with similar air mass origins and pathways during the NPF event periods at three  
7 different heights were used for the analysis in this study, as shown in Fig. 2. Accordingly, the air mass  
8 was categorized into four cases according to its origin and pathway: two affected continents including  
9 South America (Case I) and the Antarctic Peninsula (Case III) and two affected marine cases including  
10 the Weddell (Case II) and Bellingshausen Sea (Case IV).

11

## 12 **3. Results and discussion**

### 13 **3.1 Characteristics of the NPF events**

#### 14 **3.1.1 Occurrence frequency and FR of NPF events**

15 After data screening as mentioned in the previous section, 1655-days of data recorded during the  
16 observation periods from March 2009 to December 2016 were analyzed. The data including valid data  
17 were classified into two groups, NPF event days and non-event days, by using CN<sub>2.5-10</sub> concentrations  
18 measured by two CPCs. The duration of the NPF ranged from 0.6 to 14.4 h, with a mean of  $4.6 \pm 1.5$   
19 h. Only 6.1% (101 days) of the results were defined as NPF events, whereas 93.9% (1554 days) were  
20 classified as the non-NPF events (Table 2). This NPF frequency at King Sejong Station in the Antarctic  
21 Peninsula is quite low compared with those in previous studies at other mid-latitude sites (Kulmala et  
22 al., 2004; Dal Maso et al., 2005; Pierce et al., 2014; Rose et al., 2015); comparison with other sites in  
23 the Antarctic is difficult owing to the lack of long-term observed results. In addition, the monthly  
24 variation of the NPF frequency was compared as shown in Fig. 3. It is clear that the NPF number was  
25 highest during the austral summer, from December to February, whereas non-events were observed in

1 the austral winter period from June to August. Approximately 72% of the NPF occurred during the  
2 summer period, showing the highest value of 38% in January. The clear difference in the frequency of  
3 the NPF events in austral summer and winter periods [indicates that](#) solar intensity and temperature  
4 play important roles in the formation and growth of aerosol particles, [along with precursor vapors](#)  
5 [derived from marine biota activities in the Antarctica \(Virkkula et al., 2009; Weller et al., 2015; Jang](#)  
6 [et al., 2018\)](#).

7 The FR of particles ranging from 2.5 nm to 10 nm varied from  $0.16$  to  $9.88 \text{ cm}^{-3} \text{ s}^{-1}$ , with an average  
8 of  $2.79 \pm 1.05 \text{ cm}^{-3} \text{ s}^{-1}$ . Fig.4(a) shows the monthly variations in the FR over whole observation periods.  
9 The seasonal trend in the FR shows a pattern similar to that of the NPF events frequency. The FRs  
10 were the highest during the austral summer (December-February,  $3.20 \pm 1.09 \text{ cm}^{-3} \text{ s}^{-1}$ ). Those in the  
11 austral autumn period (March-May,  $1.71 \pm 0.56 \text{ cm}^{-3} \text{ s}^{-1}$ ) were similar to those of the spring period  
12 (September-November,  $1.71 \pm 0.79 \text{ cm}^{-3} \text{ s}^{-1}$ ). [Although the FR was  \$0.20 \text{ cm}^{-3} \text{ s}^{-1}\$  and air masses were](#)  
13 [originated from South America \(Case I\) in May, only one NPF event occurred.](#) In particular, the  
14 monthly maximum FR in December and the minimum in October were  $3.52 \text{ cm}^{-3} \text{ s}^{-1}$  and  $0.84 \text{ cm}^{-3} \text{ s}^{-1}$ ,  
15 respectively. The FR measured at various stations in the Antarctic and other continents are  
16 summarized in Table 3. The average level of the FR observed in this study was more than 10 times  
17 higher than that of other stations in Antarctica. Although it is difficult to directly explain the causes of  
18 the higher FR, it is likely that the method used in this study to derive the FR influenced the results.  
19 The FRs were estimated in the previous studies on the basis of the size distribution data with few  
20 minute time resolution, whereas the FR in this study was calculated by using the variation in total  
21 number concentration ( $\text{CN}_{2.5-10}$ ) data with a time resolution of 1 s. Another possible reason is the  
22 location. As shown in Table 3, the FR at a coastal region, specifically Mace Head located  
23 approximately 500 m from the coast, is higher than that reported at other sites due to the high biological  
24 activity of marine algae, which produce gaseous precursors from tidal zone and open oceans. Previous  
25 modeling research showed that the dimethyl sulfide emission in the Antarctic Peninsula during the



1 astral summer period is higher than that in other regions in Antarctica (Yu and Luo, 2010). Thus, the  
2 characteristics of the sampling site might have caused the FR to be higher than that at other site in  
3 Antarctica.

### 4 5 **3.1.2 Calculation of other parameters based on size distribution data**

6 On the basis of the size distribution results measured with a SMPS, NPF events were categorized  
7 into three NPF types, as mentioned as Sect. 2.2.2. Type C was dominant, as shown in Table 4; among  
8 all NPF event days, only two days (2.0%) were considered as Type A events. The GRs of nucleation  
9 mode particles ranged between  $0.02 \text{ nm h}^{-1}$  and  $3.09 \text{ nm h}^{-1}$ , with a mean of  $0.68 \pm 0.27 \text{ nm h}^{-1}$ . Fig.  
10 4(b) presents the monthly variation in the GR from March 2009 to December 2016. A seasonal trend  
11 in the GR is apparent, in which the maximum occurred in the summer. The GR gradually began to  
12 decrease in February and increase again in November, as shown in Fig. 4(b). The GR in January was  
13  $0.76 \pm 0.26 \text{ nm h}^{-1}$ , whereas that in November was  $0.40 \pm 0.15 \text{ nm h}^{-1}$ . [The GRs in September and](#)  
14 [October were not shown due to mechanical trouble of the instruments.](#) The GR in this study is similar  
15 to the values reported in previous studies conducted in Antarctica. For instance, Weller et al. (2015)  
16 reported that the GR at the Neumayer station varied between 0.4 and  $1.9 \text{ nm h}^{-1}$ , with an average of  
17  $0.90 \pm 0.46 \text{ nm h}^{-1}$ . However, our results are lower than those reported by Järvinen et al. (2013), who  
18 studied NPF events at Concordia station, Dome C from December 2007 to November 2009 and showed  
19 a GR of  $4.3 \text{ nm h}^{-1}$ . This discrepancy is likely attributed to the number of analyzed days. In the present  
20 study, we analyzed 86 of 101 NPF days, whereas the previous study analyzed 15 NPF days.

21 Fig. 4(c) shows a monthly variation in CS during NPF events. The CS varied from  $0.02 \times 10^{-3} \text{ s}^{-1}$   
22 to  $25.66 \times 10^{-3} \text{ s}^{-1}$ , with an average of  $(6.04 \pm 2.74) \times 10^{-3} \text{ s}^{-1}$ . The value was high in February ( $(8.17 \pm$   
23  $3.55) \times 10^{-3} \text{ s}^{-1}$ ) and a low in April ( $(2.44 \pm 0.70) \times 10^{-3} \text{ s}^{-1}$ ), as shown in Fig. 4(c). The CS measured  
24 in this study was approximately 5-10 times higher than that observed at the other Antarctic station.  
25 Weller et al. (2015), who estimated the CS using light scattering data measured from Neumayer station,

1 indicated a CS value of about  $10^{-3} \text{ s}^{-1}$ . A median CS value of  $4.0 \times 10^{-4} \text{ s}^{-1}$  in a 47-day observation period  
2 at Aboa station was reported by Kyrö et al. (2013). Järvinen et al. (2013) also showed a CS value of  
3  $1.8 \times 10^{-4} \text{ s}^{-1}$  using data of 15 days.

4 The monthly variation in the condensable vapor source rate during an NPF event is displayed in  
5 Fig. 4(d). The source rates derived were between  $0.03 \times 10^3$  and  $3.74 \times 10^5 \text{ cm}^{-3} \text{ s}^{-1}$ , with a mean source  
6 rate of  $(5.19 \pm 3.51) \times 10^4 \text{ cm}^{-3} \text{ s}^{-1}$ . The source rate of condensable vapor was maximum during the  
7 austral summer months. In particular, the maximum and minimum average values of the source rate  
8 were  $(6.40 \pm 3.43) \times 10^4 \text{ cm}^{-3} \text{ s}^{-1}$  in January and  $(1.93 \pm 0.92) \times 10^4 \text{ cm}^{-3} \text{ s}^{-1}$  in November, respectively.  
9 This source rate was higher than that measured at a coastal Antarctic station. Kulmala et al. (2005)  
10 reported that the value of source rate varied from  $0.9 \times 10^3 \text{ cm}^{-3} \text{ s}^{-1}$  to  $2.0 \times 10^4 \text{ cm}^{-3} \text{ s}^{-1}$  at the Aboa station.

11

### 12 **3.3 CCN concentration during NPF events**

13 In this section, the contribution of particle formation to the variation in CCN concentration is  
14 investigated. Although recent studies reported that number concentrations of climate-relevant particles  
15 increased during NPF events (Pierce et al., 2014; Shen et al., 2016; Rose et al., 2017), the contribution  
16 of NPF to CCN concentration was estimated by using an indirect method. The number concentrations  
17 of particles larger than 50, 80 and 100 nm were estimated by using size distribution data. That value  
18 was considered as potential CCN concentration at different supersaturation value. In this study,  
19 however, CCN concentrations at a supersaturation value of 0.4% were directly measured by CCN  
20 counter. Hourly mean CCN concentrations were compared with CN concentrations and size  
21 distribution results (Fig S3 in the Supplement). Data for only 34 days out of 101 NPF days were valid  
22 due to the CCN data availability limited by the mechanical malfunctioning of the instrument. Fig. 5  
23 shows variation in normalized values of  $\text{CN}_{2.5-10}$  and CCN concentrations as a function of time during  
24 the NPF event periods. The normalized value was calculated from  $\text{CN}_{2.5}$  and the CCN concentration  
25 at each time divided by the concentration recorded 1 h prior to the NPF event. The zero in the x-axis

1 in the figure represents the start time of the NPF event. The  $\text{CN}_{2.5-10}$  concentrations sharply increased  
2 at NPF start time and the peak concentration occurred 2 h afterward, as shown in Fig. 5. Moreover, the  
3 CCN concentrations gradually increased for 9 h. Indeed, the maximum CCN concentrations rose from  
4  $170.7 \pm 38.6 \text{ cm}^{-3}$  to  $185.6 \pm 44.6 \text{ cm}^{-3}$  during and after the NPF events, respectively, showing an increase  
5 of 9%.

6

### 7 **3.4 Effects of air mass origin on NPF events**

8 The effects of air mass origin on the NPF characteristics were also investigated by 48-h air mass  
9 back trajectory analysis. Each trajectory according to four cases can be shown in Fig. S4 in the  
10 Supplement. The frequencies of NPF, FR, GR, CS, and the source rate of condensable vapor over the  
11 whole observation period are listed in Table 5. Here, the analysis results of the NPF characteristics of  
12 air masses originating from South America (Case I) are not shown owing to low frequencies. The air  
13 masses originating from the sea (Case II and IV) were dominant during NPF event at King Sejong  
14 Station. The FRs were analogous regardless of the air mass origin and pathway, while the GR of Case  
15 III and Case IV was significantly higher than those of Case II. The lower GR should be related to the  
16 CS and the source rate of condensable vapor. In the case of the air mass originating from the Weddell  
17 Sea (Case II), the CS was higher than that of other cases, whereas the source rate of condensing vapor  
18 was lowest. The higher CS and lower source rate might indicate a decline in condensing vapor and  
19 hence a decrease in GR. Our results for the source rate of condensable vapor agree with those of a  
20 previous study by Yu and Luo (2010), discussing the role of dimethyl sulfide (DMS) emission in the  
21 NPF process in remote oceans. In their model study, the concentrations of DMS and sulfuric acid in  
22 the Bellingshausen Sea and the Antarctic Peninsula area during the austral summer season were higher  
23 than those in Weddell Sea region. In satellite-derived estimates of the biological activities, DMS  
24 produced from phytoplankton was found to be more dominant in the Bellingshausen Sea than in the  
25 Weddell Sea (Jang et al., 2018). Sulfuric acid is derived from oxidation of DMS emitted from oceans

1 (Virkkula et al., 2009). In this study, the condensable vapor was assumed to be sulfuric acid in the  
2 source rate calculations, as mentioned in Sect. 2.2.3.

3 Fig. 6 shows a comparison of the NPF characteristics depending on the origin and pathway of the  
4 air mass during the summer season. The mean CS value was high. However, in case of the air mass  
5 originating from the Bellingshausen Sea (Case IV), the GR was relatively higher than the values of air  
6 masses originated from other region. The mean value of this source rate for the air mass originating  
7 from the Weddell Sea (Case II) was similar to that from the Antarctic Peninsula (Case III), while the  
8 CS mean value was 1.7 times higher. This resulted in a low GR.

9 For air mass originating from the Bellingshausen Sea (Case IV), the seasonal properties of the  
10 parameters related to the NPF events were analyzed. As shown in Fig. 7, the mean values of FR, GR  
11 and the source rate of condensable vapor were highest during the austral summer periods. However,  
12 mean values of CS were highest during the spring period.

13

#### 14 **4. Summary**

15 In this study, the characteristics of NPF at King Sejong station in Antarctic Peninsula were  
16 investigated using a data set of eight years from March 2009 to December 2016, of total particle  
17 number concentrations and particle size distributions. The frequencies of NPF events and FR were  
18 obtained by using the data of total number concentrations, whereas GR, CS and the source rate of  
19 condensable vapor were calculated from the aerosol size distribution results. A low occurrence  
20 frequency of NPF events, at 6%, was observed, and most of the NPF events occurred during the austral  
21 summer. No NPF events were observed during the winter due to lower solar radiation and a lack of  
22 precursors for particle formation. The mean values of the FR and GR were  $2.79 \pm 1.05 \text{ cm}^{-3} \text{ s}^{-1}$  and  
23  $0.68 \pm 0.27 \text{ nm h}^{-1}$ , respectively. These results show that the FR at King Sejong Station is higher than  
24 that at other Antarctica sites, whereas the GR was relatively similar to values reported in previous  
25 studies conducted in the Antarctic. A possible reason for the lower GR can be attributed to the CS,

1 which was 5-10 times higher than that reported at other stations in Antarctica. This observation  
2 suggests that condensable vapor contributed to growth of nucleated nanoparticles and may have  
3 condensed onto pre-existing particles, hence decreasing the GR. According to 48-h backward  
4 trajectory analysis, air masses originating from oceanic areas were dominant during the NPF events.  
5 In order to investigate the contribution of the NPF events to variation in CCN concentrations at a  
6 supersaturation value of 0.4%, the CCN concentrations were compared with the CN<sub>2.5-10</sub>  
7 concentrations as a function of time. The results showed that the CCN concentrations during and after  
8 the NPF events increased approximately 9% compared with those measured before the event. This  
9 study is the first to report the characteristics of NPF in the Antarctic Peninsula. However, further  
10 research is need to understand the chemical characteristics of aerosol particles and the chemical  
11 composition of precursors during NPF events to fully understand the NPF for this region.

12

### 13 **Author contributions**

14 JK and YJY designed the study, YG, JHC, HJK, KTP, JP, and BYL analysed aerosol data. JK and  
15 YJY prepared the manuscript with contributions from all co-authors.

16

### 17 **Acknowledgements**

18 We would like to thank the many technicians and scientists of the overwintering crews. This work was  
19 supported by the KOPRI project (PE19010) and a Korea Grant from the Korean Government (MSIP)  
20 (NRF-2016M1A5A1901769) (KOPRI-PN19081).

21

### 22 **References**

- 23 Albrecht, B. A.: Aerosols, cloud microphysics, and fractional cloudiness, *Science*, 245, 1227-1230,  
24 10.1126/science.245.4923.1227, 1989.
- 25 Anttila, T., Brus, D., Jaatinen, A., Hyvärinen, A.-P., Kivekäs, N., Romakkaniemi, S., Komppula, M.,  
26 and Lihavainen, H.: Relationships between particles, cloud condensation nuclei and cloud droplet  
27 activation during the third Pallas Cloud Experiment, *Atmos. Chem. Phys.*, 12, 11435–11450,  
28 <https://doi.org/10.5194/acp-12-11435-2012>, 2012.

- 1 Asmi, E., Frey, A., Virkkula, A., Ehn, M., Manninen, H. E., Timonen, H., Tolonen-Kivimäki, O.,  
2 Aurela, M., Hillamo, R., and Kulmala, M.: Hygroscopicity and chemical composition of antarctic  
3 sub-micrometre aerosol particles and observations of new particle formation, *Atmos. Chem. Phys.*,  
4 10, 4253-4271, 10.5194/acp-10-4253-2010, 2010.
- 5 Barbaro, E., Padoan, S., Kirchgeorg, T., Zangrando, R., Toscano, G., Barbante, C., and Gambaro, A.:  
6 Particle size distribution of inorganic and organic ions in coastal and inland Antarctic aerosol,  
7 *Environ. Sci. Pollut. Res.*, 24, 2724-2733, 10.1007/s11356-016-8042-x, 2017.
- 8 Bianchi, F., Tröstl, J., Junninen, H., Frege, C., Henne, S., Hoyle, C. R., Molteni, U., Herrmann, E.,  
9 Adamov, A., Bukowiecki, N., Chen, X., Duplissy, J., Gysel, M., Hutterli, M., Kangasluoma, J.,  
10 Kontkanen, J., Kürten, A., Manninen, H. E., Münch, S., Peräkylä, O., Petäjä, T., Rondo, L.,  
11 Williamson, C., Weingartner, E., Curtius, J., Worsnop, D. R., Kulmala, M., Dommen, J., and  
12 Baltensperger, U.: New particle formation in the free troposphere: A question of chemistry and  
13 timing, *Science*, 352, 1109-1112, 10.1126/science.aad5456, 2016.
- 14 Carslaw, K. S., Lee, L. A., Reddington, C. L., Pringle, K. J., Rap, A., Forster, P. M., Mann, G. W.,  
15 Spracklen, D. V., Woodhouse, M. T., Regayre, L. A., and Pierce, J. R.: Large contribution of natural  
16 aerosols to uncertainty in indirect forcing, *Nature*, 503, 67-71, 10.1038/nature12674, 2013.
- 17 Dal Maso, M.: Condensation and coagulation sinks and formation of nucleation mode particles in  
18 coastal and boreal forest boundary layers, *J. Geophys. Res.*, 107, 10.1029/2001jd001053, 2002.
- 19 Dal Maso, M., Kulmala, M., Riipinen, I., Wagner, R., Hussein, T., Aalto, P. P., and Lehtinen, K. E. J.:  
20 Formation and growth of fresh atmospheric aerosols: Eight years of aerosol size distribution data  
21 from SMEAR II, Hyytiälä, Finland, *Boreal Environ. Res.*, 10, 323-336, 2005.
- 22 [Dall'Osto, M., Beddows, D. C. S., Tunved, P., Krejci, R., Ström, J., Hansson, H. C., Yoon, Y. J., Park,](#)  
23 [K. T., Becagli, S., Udisti, R., Onasch, T., Ódowd, C. D., Simó, R., and Harrison, R. M.: Arctic sea](#)  
24 [ice melt leads to atmospheric new particle formation, \*Sci. Rep.\*, 7, 10.1038/s41598-017-03328-1,](#)  
25 [2017.](#)
- 26 Fuchs, N. A., and Sutugin, A. G.: *Highly Dispersed Aerosols*, Ann Arbor Science Publ., Ann Arbor,  
27 Michigan, 1970.
- 28 Grenfell, J. L., Harrison, R. M., Allen, A. G., Shi, J. P., Penkett, S. A., O'Dowd, C. D., Smith, M. H.,  
29 Hill, M. K., Robertson, L., Hewitt, C. N., Davison, B., Lewis, A. C., Creasey, D. J., Heard, D. E.,  
30 Hebestreit, K., Alicke, B., and James, J.: An analysis of rapid increases in condensation nuclei  
31 concentrations at a remote coastal site in western Ireland, *J. Geophys. Res.: Atmos.*, 104, 13771-  
32 13780, 1999.
- 33 Humphries, R. S., Schofield, R., Keywood, M. D., Ward, J., Pierce, J. R., Gionfriddo, C. M., Tate, M.  
34 T., Krabbenhoft, D. P., Galbally, I. E., Molloy, S. B., Klekociuk, A. R., Johnston, P. V., Kreher, K.,  
35 Thomas, A. J., Robinson, A. D., Harris, N. R. P., Johnson, R., and Wilson, S. R.: Boundary layer  
36 new particle formation over East Antarctic sea ice - Possible Hg-driven nucleation?, *Atmos. Chem.*  
37 *Phys.*, 15, 13339-13364, 10.5194/acp-15-13339-2015, 2015.
- 38 Humphries, R. S., Klekociuk, A. R., Schofield, R., Keywood, M. D., Ward, J., and Wilson, S. R.:  
39 Unexpectedly high ultrafine aerosol concentrations above East Antarctic sea ice, *Atmos. Chem.*  
40 *Phys.*, 16, 2185-2206, 10.5194/acp-16-2185-2016, 2016.
- 41 Jang, E., Park, K.-T., Yoon, Y. J., Kim, T.-W., Hong, S.-B., Becagli, S., Traversi, R., Kim, J., and Gim,  
42 Y.: New particle formation events observed at the King Sejong Station, Antarctic Peninsula – Part  
43 2: Link with the oceanic biological activities, Manuscript submitted for publication, 2018.

1 IPCC: Climate change 2013: The physical science basis, Intergovernmental panel on Climate Change,  
2 Cambridge University Press, New York, USA, 571-740, 2013.

3 Ito, T.: Size distribution of Antarctic submicron aerosols, *Tellus Ser. B*, 45 B, 145-159, 1993.

4 Järvinen, E., Virkkula, A., Nieminen, T., Aalto, P. P., Asmi, E., Lanconelli, C., Busetto, M., Lupi, A.,  
5 Schioppo, R., Vitale, V., Mazzola, M., Petäjä, T., Kerminen, V. M., and Kulmala, M.: Seasonal  
6 cycle and modal structure of particle number size distribution at Dome C, Antarctica, *Atmos. Chem.*  
7 *Phys.*, 13, 7473-7487, 10.5194/acp-13-7473-2013, 2013.

8 Keil, A., and Wendisch, M.: Bursts of Aitken mode and ultrafine particles observed at the top of  
9 continental boundary layer clouds, *J. Aerosol. Sci.*, 32, 649-660, 10.1016/s0021-8502(00)00102-6,  
10 2001.

11 Kim, J., Yoon, Y. J., Gim, Y., Kang, H. J., Choi, J. H., Park, K.-T., and Lee, B. Y.: Seasonal variations  
12 in physical characteristics of aerosol particles at the King Sejong Station, Antarctic Peninsula,  
13 *Atmos. Chem. Phys.*, 17, 12985-12999, 10.5194/acp-17-12985-2017, 2017.

14 Kim, J. S., Kim, Y. J., and Park, K.: Measurements of hygroscopicity and volatility of atmospheric  
15 ultrafine particles in the rural Pearl River Delta area of China, *Atmos. Environ.*, 45, 4661-4670,  
16 2011.

17 Komppula, M., Lihavainen, H., Hatakka, J., Paatero, J., Aalto, P., Kulmala, M., and Viisanen, Y.:  
18 Observations of new particle formation and size distributions at two different heights and  
19 surroundings in subarctic area in northern Finland, *J. Geophys. Res. D: Atmos.*, 108, AAC 12-11  
20 AAC 12-11, 2003.

21 Kontkanen, J., Lehtipalo, K., Ahonen, L., Kangasluoma, J., Manninen, H. E., Hakala, J., Rose, C.,  
22 Sellegri, K., Xiao, S., Wang, L., Qi, X., Nie, W., Ding, A., Yu, H., Lee, S., Kerminen, V. M., Petäjä,  
23 T., and Kulmala, M.: Measurements of sub-3nm particles using a particle size magnifier in different  
24 environments: From clean mountain top to polluted megacities, *Atmos. Chem. Phys.*, 17, 2163-  
25 2187, 10.5194/acp-17-2163-2017, 2017.

26 Kulmala, M., Dal Maso, M., Mäkelä, J. M., Pirjola, L., Väkevä, M., Aalto, P., Miikkulainen, P., Hämeri,  
27 K., and O'Dowd, C. D.: On the formation, growth and composition of nucleation mode particles,  
28 *Tellus Ser. B*, 53, 479-490, 2001.

29 Kulmala, M., Vehkamäki, H., Petäjä, T., Dal Maso, M., Lauri, A., Kerminen, V. M., Birmili, W., and  
30 McMurry, P. H.: Formation and growth rates of ultrafine atmospheric particles: A review of  
31 observations, *J. Aerosol. Sci.*, 35, 143-176, 10.1016/j.jaerosci.2003.10.003, 2004.

32 Kulmala, M., Petäjä, T., Mönkkönen, P., Koponen, I. K., Dal Maso, M., Aalto, P. P., Lehtinen, K. E. J.,  
33 and Kerminen, V. M.: On the growth of nucleation mode particles: source rates of condensable  
34 vapor in polluted and clean environments, *Atmos. Chem. Phys.*, 5, 409-416, 10.5194/acp-5-409-  
35 2005, 2005.

36 Kyrö, E. M., Kerminen, V. M., Virkkula, A., Dal Maso, M., Parshintsev, J., Ruíz-Jimenez, J., Forsström,  
37 L., Manninen, H. E., Riekkola, M. L., Heinonen, P., and Kulmala, M.: Antarctic new particle  
38 formation from continental biogenic precursors, *Atmos. Chem. Phys.*, 13, 3527-3546, 10.5194/acp-  
39 13-3527-2013, 2013.

40 Nguyen, Q. T., Glasius, M., Sørensen, L. L., Jensen, B., Skov, H., Birmili, W., Wiedensohler, A.,  
41 Kristensson, A., Nøjgaard, J. K., and Massling, A.: Seasonal variation of atmospheric particle  
42 number concentrations, new particle formation and atmospheric oxidation capacity at the high  
43 Arctic site Villum Research Station, Station Nord, *Atmos. Chem. Phys.*, 16, 11319-11336,

1 10.5194/acp-16-11319-2016, 2016.

2 O'Dowd, C. D., Hämeri, K., Mäkelä, J., Väkeva, M., Aalto, P., De Leeuw, G., Kunz, G. J., Becker, E.,  
3 Hansson, H. C., Allen, A. G., Harrison, R. M., Berresheim, H., Kleefeld, C., Geever, M., Jennings,  
4 S. G., and Kulmala, M.: Coastal new particle formation: Environmental conditions and aerosol  
5 physicochemical characteristics during nucleation bursts, *J. Geophys. Res.: Atmos.*, 107,  
6 10.1029/2000JD000206, 2002.

7 Park, J., Sakurai, H., Vollmers, K., and McMurry, P. H.: Aerosol size distributions measured at the  
8 South Pole during ISCAT, *Atmos. Environ.*, 38, 5493-5500, 10.1016/j.atmosenv.2002.12.001, 2004.

9 Park, K., Kim, J. S., and Seung, H. P.: Measurements of hygroscopicity and volatility of atmospheric  
10 ultrafine particles during ultrafine particle formation events at urban, industrial, and coastal sites,  
11 *Environ. Sci. Technol.*, 43, 6710-6716, 2009.

12 Pierce, J. R., and Adams, P. J.: Efficiency of cloud condensation nuclei formation from ultrafine  
13 particles, *Atmos. Chem. Phys.*, 7, 1367-1379, 10.5194/acp-7-1367-2007, 2007.

14 Pierce, J. R., Westervelt, D. M., Atwood, S. A., Barnes, E. A., and Leaitch, W. R.: New-particle  
15 formation, growth and climate-relevant particle production in Egbert, Canada: analysis from 1 year  
16 of size-distribution observations, *Atmos. Chem. Phys.*, 14, 8647-8663, 10.5194/acp-14-8647-2014,  
17 2014.

18 Rose, C., Sellegri, K., Velarde, F., Moreno, I., Ramonet, M., Weinhold, K., Krejci, R., Andrade, M.,  
19 Wiedensohler, A., and Laj, P.: Frequent nucleation events at the high altitude station of Chacaltaya  
20 (5240m a.s.l.), Bolivia, *Atmos. Environ.*, 102, 18-29, 10.1016/j.atmosenv.2014.11.015, 2015.

21 Rose, C., Sellegri, K., Moreno, I., Velarde, F., Ramonet, M., Weinhold, K., Krejci, R., Andrade, M.,  
22 Wiedensohler, A., Ginot, P., and Laj, P.: CCN production by new particle formation in the free  
23 troposphere, *Atmos. Chem. Phys.*, 17, 1529-1541, 10.5194/acp-17-1529-2017, 2017.

24 Shen, X., Sun, J., Zhang, X., Zhang, Y., Zhang, L., and Fan, R.: Key features of new particle formation  
25 events at background sites in China and their influence on cloud condensation nuclei, *Front.*  
26 *Environ. Sci. Eng.*, 10, 05, 10.1007/s11783-016-0833-2, 2016.

27 Spracklen, D. V., Carslaw, K. S., Kulmala, M., Kerminen, V. M., Mann, G. W., and Sihto, S. L.: The  
28 contribution of boundary layer nucleation events to total particle concentrations on regional and  
29 global scales, *Atmos. Chem. Phys.*, 6, 5631-5648, 10.5194/acp-6-5631-2006, 2006.

30 Stein, A. F., Draxler, R. R., Rolph, G. D., Stunder, B. J. B., Cohen, M. D., and Ngan, F.: NOAA's hysplit  
31 atmospheric transport and dispersion modeling system, *Bull. Amer. Meteorol. Soc.*, 96, 2059-2077,  
32 10.1175/bams-d-14-00110.1, 2015.

33 Twomey, S.: The Influence of Pollution on the Shortwave Albedo of Clouds, *J. Atmos. Sci.*, 34, 1149-  
34 1152, 10.1175/1520-0469(1977)034<1149:Tiopot>2.0.Co;2, 1977.

35 Virkkula, A., Asmi, E., Teinilä, K., Frey, A., Aurela, M., Timonen, H., Mäkelä, T., Samuli, A., Hillamo,  
36 R., Aalto, P. P., Kirkwood, S., and Kulmala, M.: Review of aerosol research at the Finnish Antarctic  
37 research station Aboa and its surroundings in Queen Maud Land, Antarctica, *Geophysica*, 45, 163-  
38 181, 2009.

39 Warren, D. R., and Seinfeld, J. H.: Prediction of aerosol concentrations resulting from a burst of  
40 nucleation, *J Colloid Interf. Sci.*, 105, 136-142, [https://doi.org/10.1016/0021-9797\(85\)90356-X](https://doi.org/10.1016/0021-9797(85)90356-X),  
41 1985.

42 Weingartner, E., Nyeki, S., and Baltensperger, U.: Seasonal and diurnal variation of aerosol size  
43 distributions ( $10 < D < 750$  nm) at a high-alpine site (Jungfraujoch 3580 m asl), *J. Geophys. Res.:*



1 Atmos., 104, 26809-26820, 1999.

2 Weller, R., Schmidt, K., Teinilä, K., and Hillamo, R.: Natural new particle formation at the coastal  
3 Antarctic site Neumayer, *Atmos. Chem. Phys.*, 15, 11399-11410, 10.5194/acp-15-11399-2015,  
4 2015.

5 Willis, M. D., Burkart, J., Thomas, J. L., Köllner, F., Schneider, J., Bozem, H., Hoor, P. M., Aliabadi,  
6 A. A., Schulz, H., Herber, A. B., Leaitch, W. R., and Abbatt, J. P. D.: Growth of nucleation mode  
7 particles in the summertime Arctic: A case study, *Atmos. Chem. Phys.*, 16, 7663-7679,  
8 10.5194/acp-16-7663-2016, 2016.

9 Woo, K. S., Chen, D. R., Pui, D. Y. H., and McMurry, P. H.: Measurement of Atlanta aerosol size  
10 distributions: Observations of ultrafine particle events, *Aerosol Sci. Technol.*, 34, 75-87, 2001.

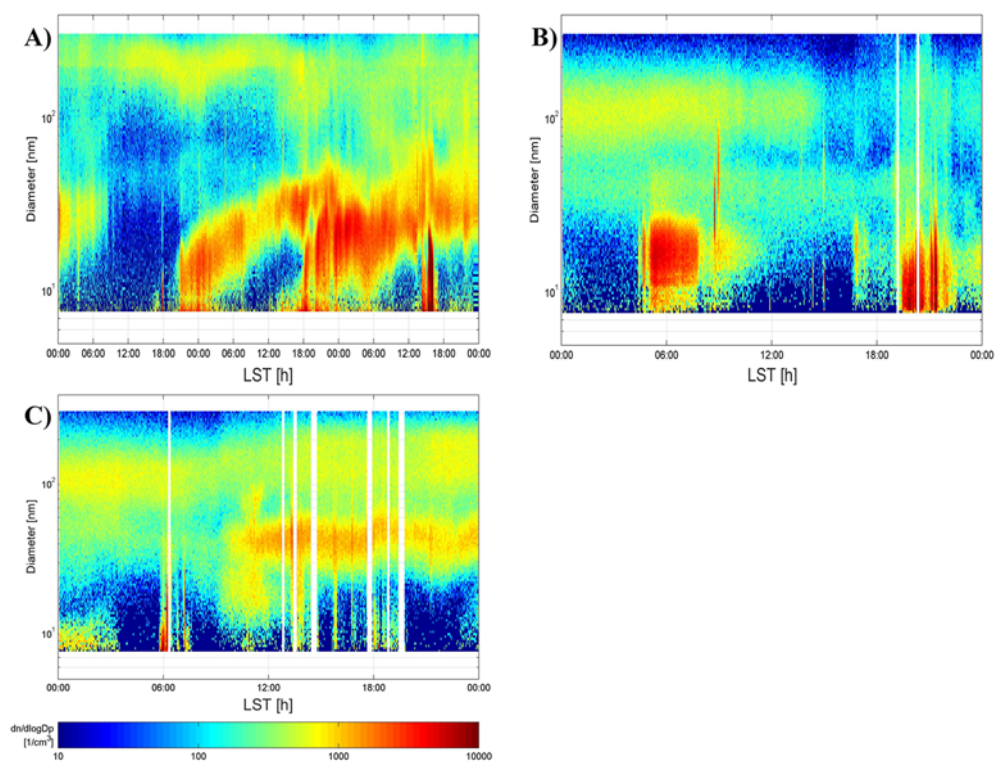
11 Yli-Juuti, T., Riipinen, I., Aalto, P. P., Nieminen, T., Maenhaut, W., Janssens, I. A., Claeys, M., Salma,  
12 I., Ocskay, R., Hoffer, A., Imre, K., and Kulmala, M.: Characteristics of new particle formation  
13 events and cluster ions at K-pusztá, Hungary, *Boreal Environ. Res.*, 14, 683-698, 2009.

14 Yoon, Y. J., O'Dowd, C. D., Jennings, S. G., and Lee, S. H.: Statistical characteristics and predictability  
15 of particle formation events at Mace Head, *J. Geophys. Res.: Atmos.*, 111, 10.1029/2005JD006284,  
16 2006.

17 Yu, F., and Luo, G.: Oceanic dimethyl sulfide emission and new particle formation around the coast of  
18 antarctica: A modeling study of seasonal variations and comparison with measurements,  
19 *Atmosphere*, 1, 34-50, 10.3390/atmos1010034, 2010.

20  
21

1



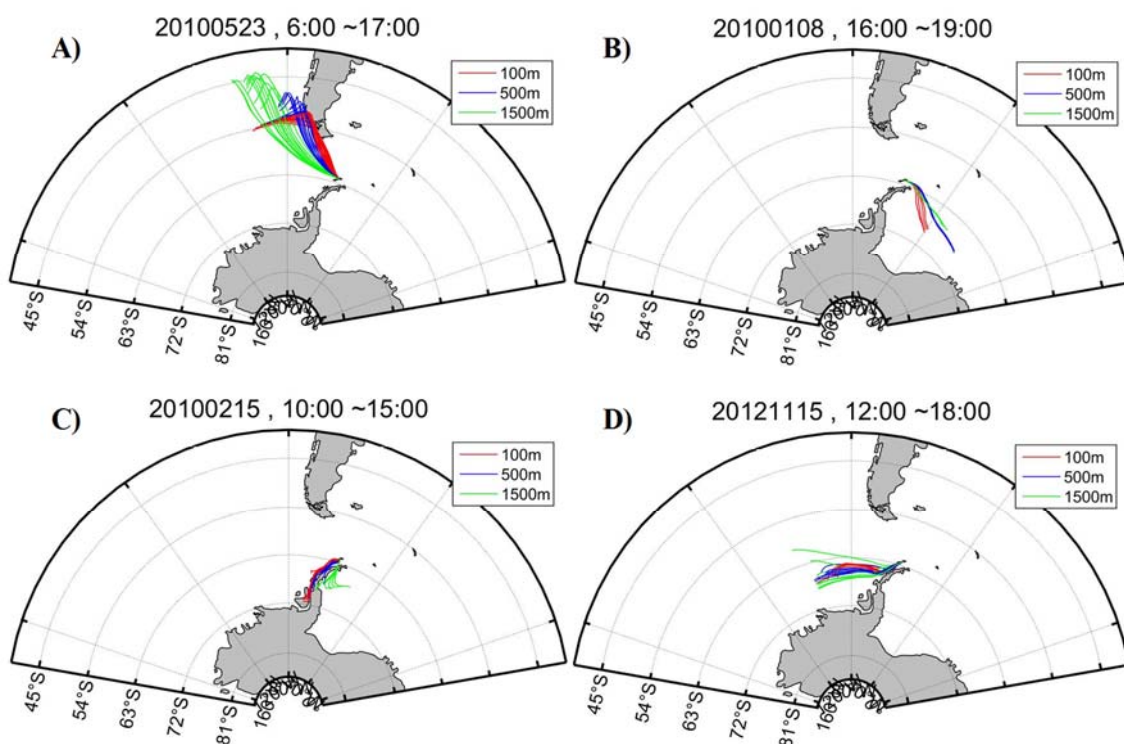
2

3

4 Figure 1. Example of types of the NPF based on the SMPS data. (a) type A (18 January 2011-20 January 2011),  
5 (b) type B (13 January 2015) and (c) type C (9 January 2015). Type A is days when the formation and growth  
6 of nanoparticles should be clear. Type B is days when the formation occurred but growth was not clear. Type C  
7 is days when it cannot be said whether there is an event or not.

8

1



2

3

4 Figure 2. Example of the four cases considering to the air mass origin and pathway: (a) South  
5 America, (b) Weddell Sea, (c) Antarctic Peninsula, and (d) Bellingshausen Sea. Typical 48-h air mass  
6 backward trajectories were analyzed, ending at heights of 100m (Red line), 500m (Blue line) and  
7 1500m (Green line) above the ground level of the sampling site.

8

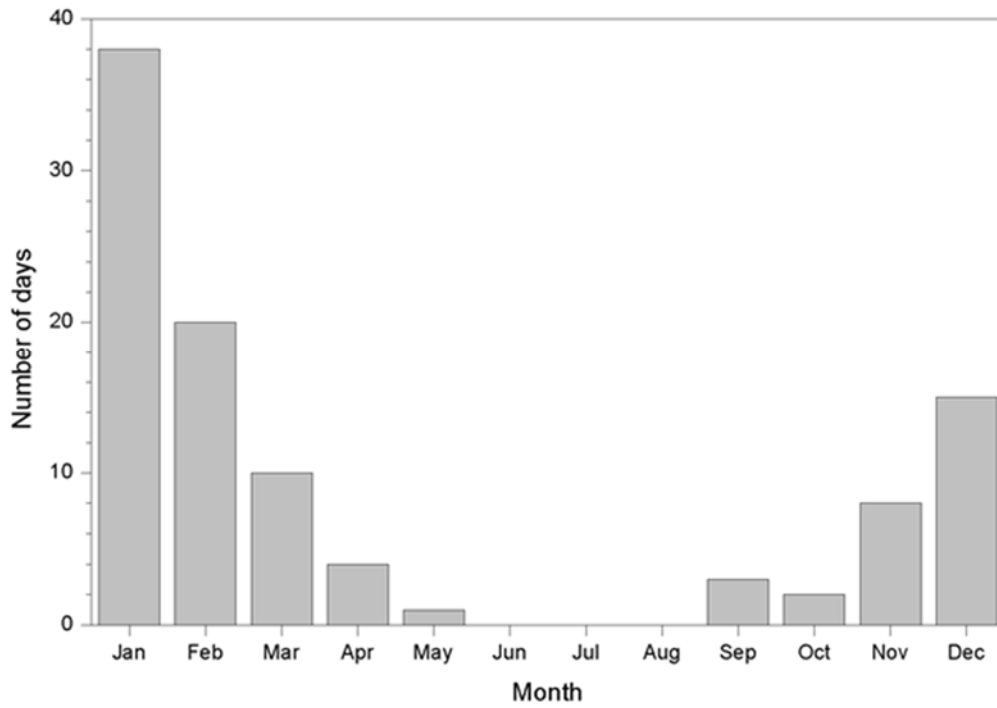
9

10

11

12

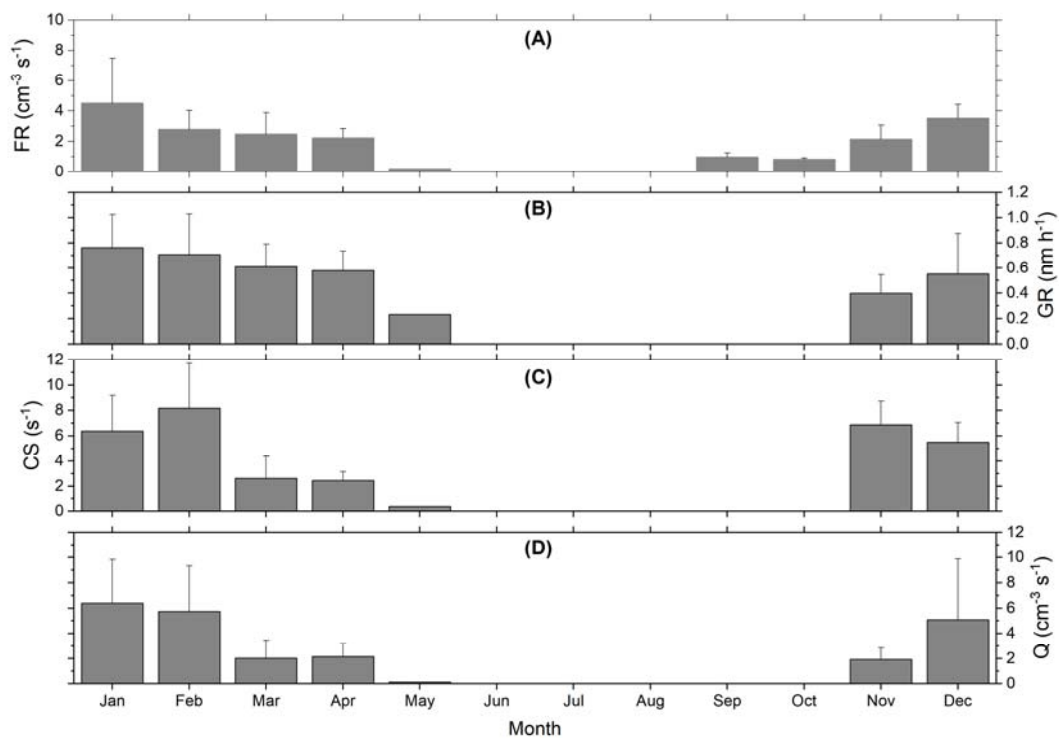
1  
2



3  
4  
5  
6  
7

Figure 3. Monthly variation in the number of NPF days between March 2009 and December 2016.

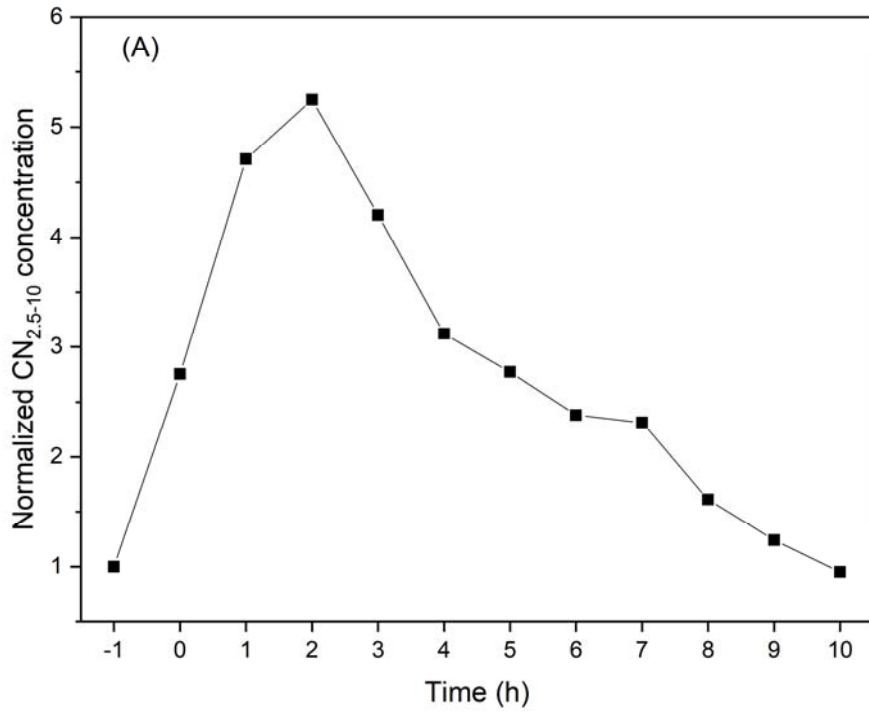
1  
2



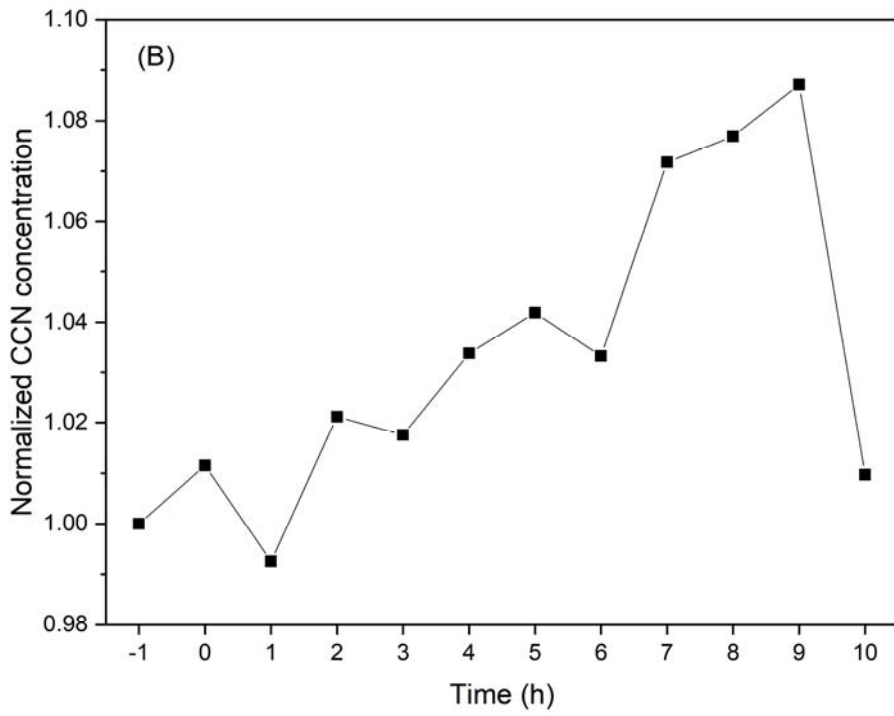
3  
4  
5  
6  
7  
8  
9  
10

Figure 4. Monthly variations of (a) the formation rates (FR), (b) the growth rates (GR) of nucleation mode particles ranging from 10 nm to 25 nm, (c) the condensation sink (CS), and (d) the source rate of condensable vapor (Q). The error bars represent a standard deviation. The GRs in September and October were not shown due to mechanical trouble of the instruments.

1



2

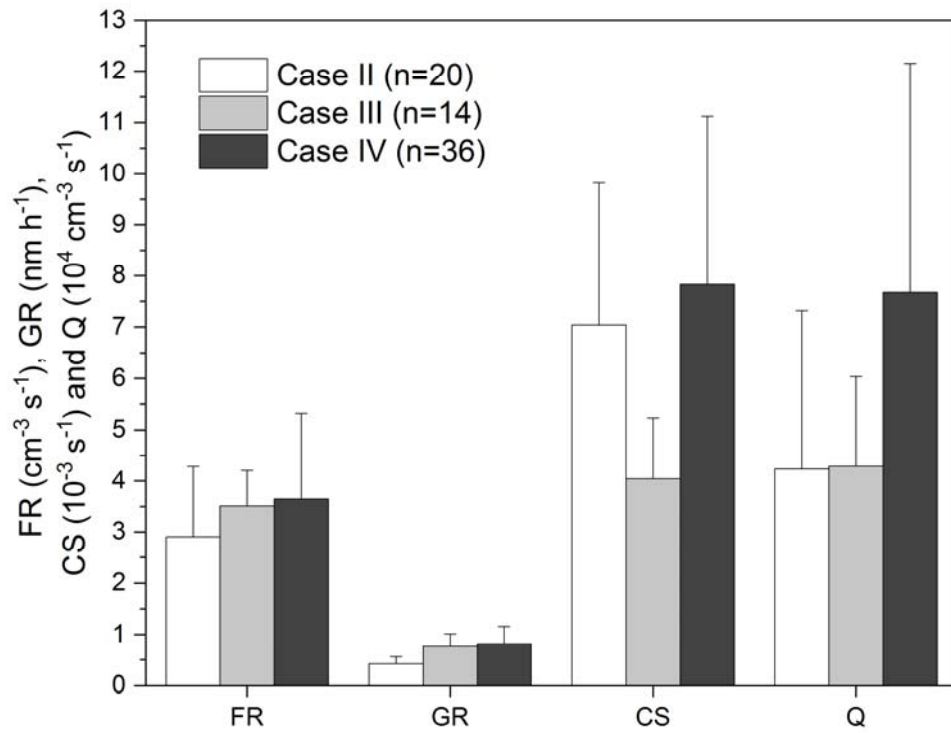


3

4

5 Figure 5. Variation in normalized (a)  $CN_{2.5-10}$  and (b) CCN concentration with time. The zero in the x-  
6 axis indicates the start time of the NPF events.

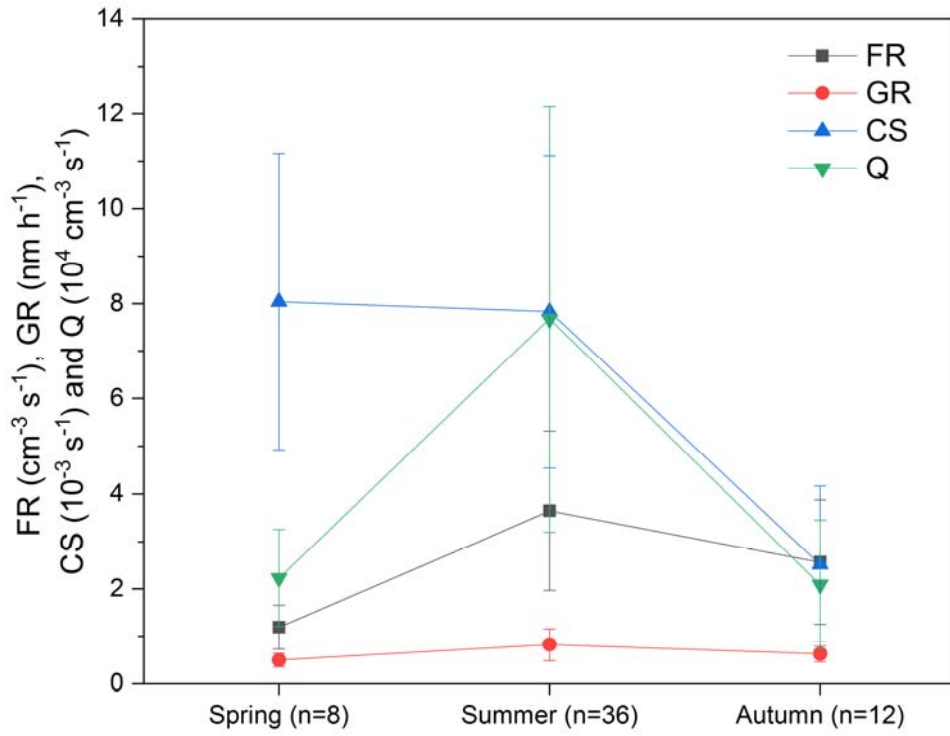
1  
2



3  
4  
5  
6  
7  
8  
9

Figure 6. Comparison of NPF characteristics including the formation rate (FR), growth rate (GR), condensation sink (CS) and source rate of condensable vapors (Q) depending on the origins and pathway of air masses during the astral summer period. The error bars represent standard deviation.

1  
2



3  
4  
5  
6  
7  
8  
9  
10

Figure 7. Seasonal characteristics of parameters related to NPF events in which the air masses originated from the Bellingshausen Sea. FR, GR, CS, and Q refer to formation rate, growth rate, condensation sink, and source rate of condensing vapor, respectively. The error bars represent standard deviation.



1

2 Table 1. Summary of data acquisition rate for each instrument during the analysis periods

Measurement parameter	Instrument	Data acquisition rate(%)
Number concentration of particle larger than 2.5 nm	CPC (TSI 3776)	80.7
Number concentration of particle larger than 10 nm	CPC (TSI 3772)	79.5
Size distribution	SMPS	40.3
CCN concentrations	CCNC	36.4

3

4

5

6 Table 2. Event statistics classified by using total concentration data obtained from two CPCs

	Days	Percentage of total days
NPF events	101	6.1
Non events	1554	93.9
Total	1655	

7

1 Table 3. Summary of the formation rates observed at different sampling site in Antarctica and in other continents. DMPS, SMPS, and CPC mean  
 2 differential mobility particle sizer, scanning mobility particle sizer, and condensation particle counter, respectively.

3

Site	Period	Method	Formation rates (cm <sup>-3</sup> s <sup>-1</sup> )		References
King Sejong (Antarctic Peninsula)	03/2009 ~ 12/2016	Two CPCs (TSI 3772 & TSI 3776)	J <sub>2.5-10</sub>	2.79	This study
Syowa (Antarctica)	08/1978 ~ 12/1978		J <sub>10</sub>	3.8×10 <sup>-4</sup>	Ito, 1993
Dome C (Antarctica)	12/2007 ~ 11/2009	DMPS	J <sub>10</sub>	0.038	Järvinen et al., 2013
Aboa (Antarctica)	01/2010	DMPS	J <sub>10</sub>	0.003 ~ 0.3	Kyrö et al., 2013
Neumayer (Antarctica)	20/01/2012 ~ 26/03/2012 01/02/2014 ~ 30/04/2014	SMPS	J <sub>3-25</sub>	0.02 ~ 0.1	Weller et al., 2015
Värriö (Sub Arctic)	12/1997 ~ 07/2001	DMPS	J <sub>10</sub>	0.38	Dal Maso, 2002
Hyytiälä (Rural)	1996 ~ 2003	DMPS	J <sub>3-25</sub>	0.61	Dal Maso et al., 2005
Mace Head (Coastal)	1996 ~ 1997	Two CPCs (TSI 3022 & TSI 3025)	J <sub>3-10</sub>	10 <sup>2</sup> ~ 10 <sup>4</sup>	Grenfell et al., 1999
Jungfrauoch (Remote)	03/1997 ~ 05/1998	SMPS	J <sub>10</sub>	0.14	Weingartner et al., 1999
Dresden area (Rural)	1996 ~ 1998	Two CPCs (UCPC & CPC)	J <sub>10</sub>	110	Keil and Wendisch, 2001
Atlanta (Urban)	08/1998 ~ 08/1999	Nano-SMPS	J <sub>3</sub>	10 ~ 15	Woo et al., 2001
Shangdianzi (Rural)	03/2008 ~ 12/2013	DMPS	J <sub>3</sub>	6.3	Shen et al., 2016

Table 4. NPF event classification statistics using size distribution results. Type A refers to days in which the formation and growth of particles were clear. Type B refer to days in which the formation occurred but the growth was not clear. Type C refers to days in which the event occurrence was unclear.

	Days	Percentage of NPF days
Type A	2	2.0
Type B	37	36.6
Type C	62	61.4
Total	101	

Table 5. Summary of NPF characteristic statics depending on the air mass origin. FR is the formation rate, GR is the growth rate, CS is the condensation sink, and Q is the source rate of condensable vapor. Case I, Case II, Case III, and Case IV refer to the origin and pathway of air masses from South America, the Weddell Sea, the Antarctic Peninsula, and the Bellingshausen Sea, respectively.

NPF days		FR ( $\text{cm}^{-3} \text{ s}^{-1}$ )	GR ( $\text{nm h}^{-1}$ )	CS ( $10^{-3} \text{ s}^{-1}$ )	Q ( $10^4 \text{ cm}^{-3} \text{ s}^{-1}$ )
Case I	3				
Case II	24	$2.81 \pm 1.29$	$0.41 \pm 0.15$	$6.95 \pm 2.65$	$3.87 \pm 2.90$
Case III	16	$3.10 \pm 0.80$	$0.77 \pm 0.25$	$4.19 \pm 1.30$	$4.29 \pm 1.75$
Case IV	56	$3.08 \pm 1.55$	$0.76 \pm 0.30$	$6.79 \pm 3.20$	$6.20 \pm 4.08$

*Supplement of*

**New particle formation observed at King Sejong Station, Antarctic Peninsula – Part 1: Physical characteristics and contribution to cloud condensation nuclei**

Jaeseok Kim et al.

Correspondence to: Young Jun Yoon ([yjyoon@kopri.re.kr](mailto:yjyoon@kopri.re.kr))

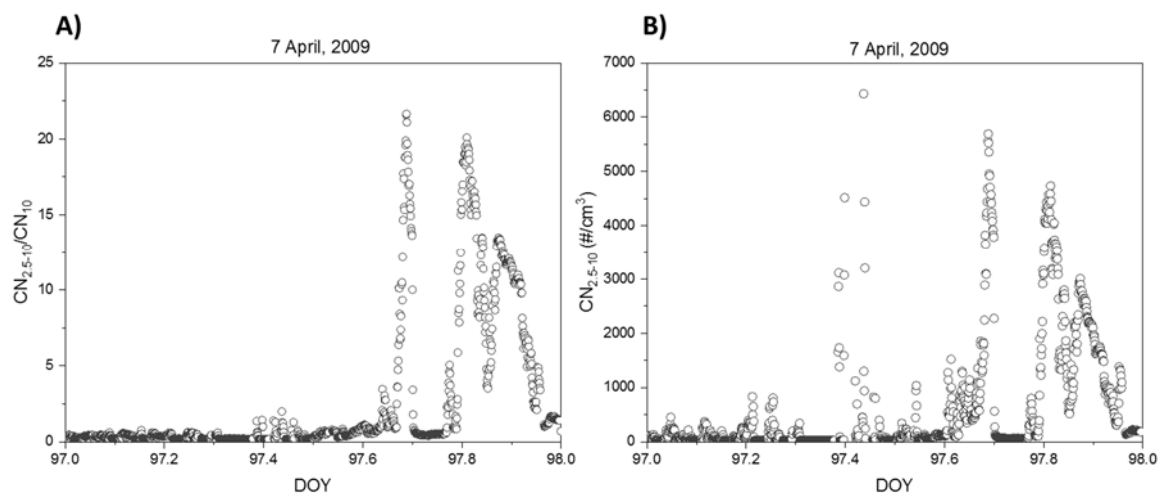


Figure S1. Example for estimation of the formation rate during NPF event on 7 April 2009: (a)  $CN_{2.5-10}/CN_{10}$  and (b)  $CN_{2.5-10}$  concentration with 1-minute time resolution.

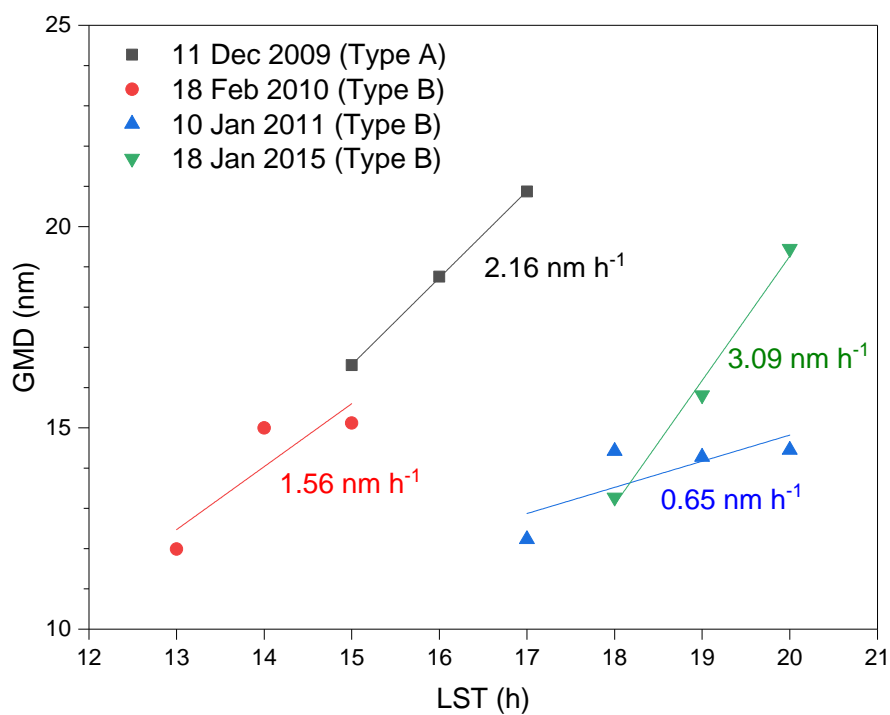


Figure S2. Geometric mean diameter (GMD) of particles ranging from 10 nm to 25 nm as a function of the time: the growth rate ( $\text{nm h}^{-1}$ ) was calculated as the regression slope. The LST means local standard time.

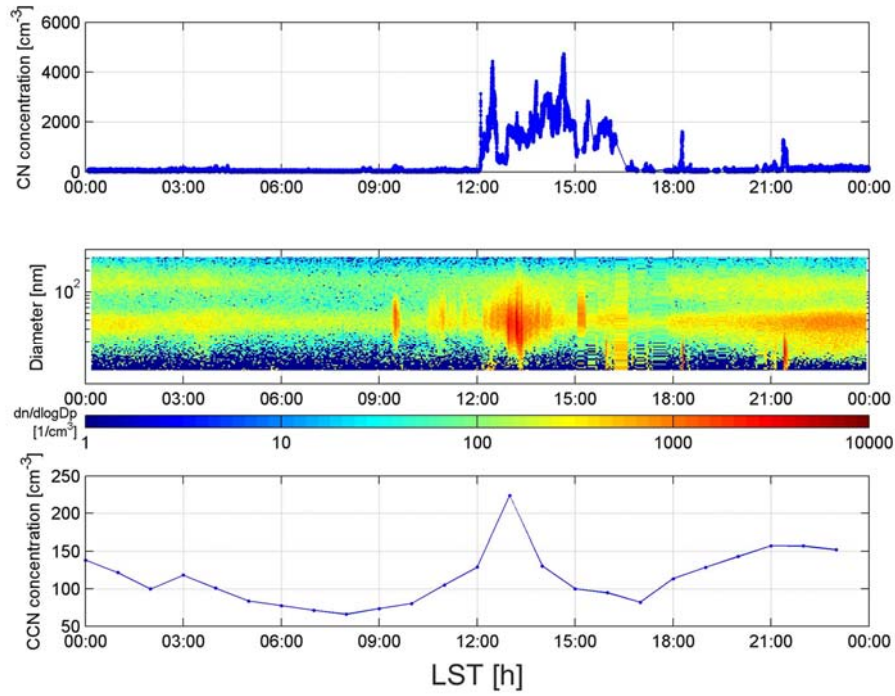


Figure S3. Example of comparison among CN concentrations from CPC data (upper panel), size distribution from SMPS data (middle panel) and hourly mean CCN concentration (bottom panel) at 0.4% supersaturation value as a function of time on 30 March 2009.

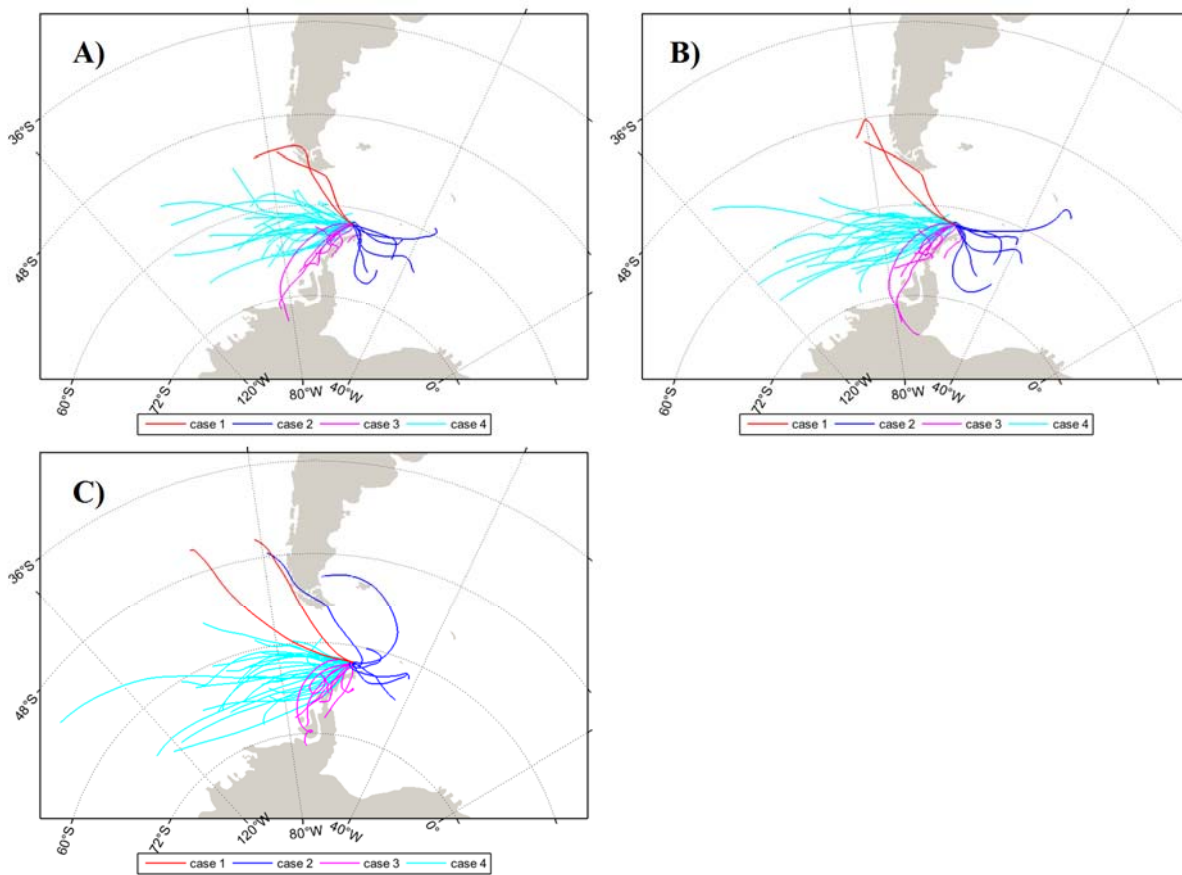


Figure S4. 48-h air mass backward trajectories at height of (a) 100m, (b) 500 m and (c) 1500 m above the ground level of the sampling site. Because 2-day trajectories can't be classified in four cases based on category method in this study, 99-day trajectories were shown. Red, blue, pink and cyan colored line indicate that air masses originated from the South America area (Case I), Weddell Sea (Case II), Antarctic Peninsula area (Case III) and Bellingshausen Sea (Case IV), respectively.